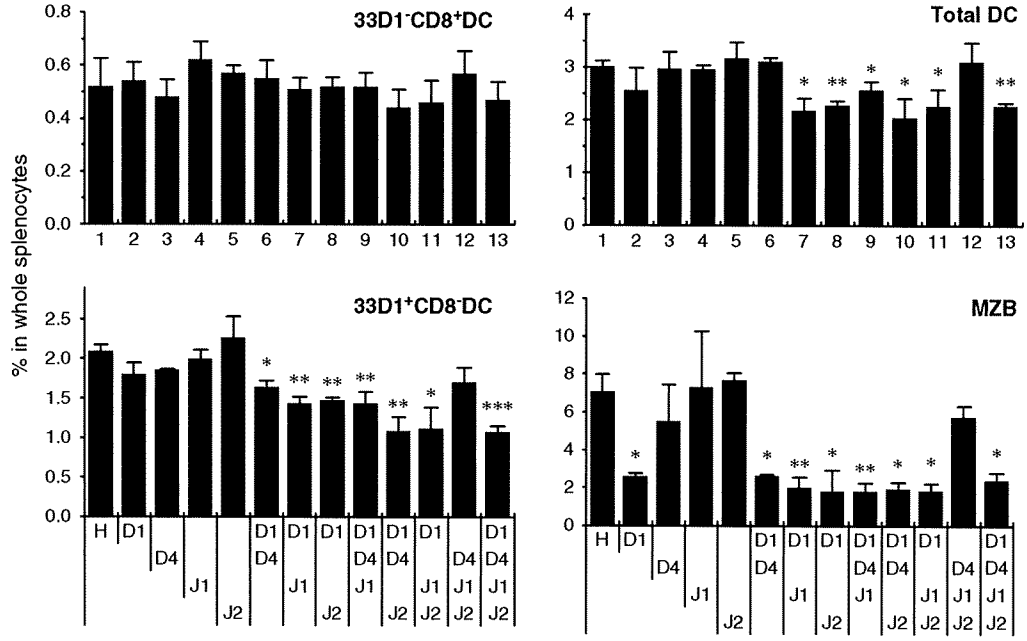

Fig. 3. Effects of anti-Notch ligand mAbs on the maintenance of CD8⁻ DCs. Mice were treated with control hamster IgG (H) or the indicated combination of mAbs (D1, HMD1-5; D4, HMD4-2; J1, HMJ1-29; J2, HMJ2-1). The percentages of $CD11c^{high}$/33D1⁺/CD8⁻ (33D1⁺CD8⁻ DC), $CD11c^{high}$/33D1⁻/CD8⁺ (33D1⁻CD8⁺ DC) and $CD11c^{high}$ (total DC) cells among whole splenocytes and the percentage of MZ B cells (B220⁺/$CD21^{hi}$/$CD23^{lo/-}$) among total B cells (B220⁺) were analyzed by flow cytometry. Data were represented as the mean ± SD of three mice in each group. Similar results were obtained in two independent experiments. Data were analyzed statistically using unpaired Student's *t*-test. $*P < 0.05$, $**P < 0.01$, $***P < 0.001$ versus hamster IgG-treated control mice.

R848 (Alexis) or 1 μg ml^{-1} LPS (Sigma, St Louis, MO, USA) in DMEM/10% FCS (Nissui, Tokyo, Japan) for 2 h. Then, add GolgiPlug (BD Biosciences) and incubate for additional 4 h. Cells were stained for surface markers, fixed, permeabilized and stained with PE-conjugated anti-mouse IL-12 (Biolegend).

Immunohistological staining

Tissue samples of spleen were frozen in optimal cutting temperature compound (SAKURA, Tokyo, Japan) and were cut into 3-μm sections. After being air-dried, sections were fixed in acetone, blocked with control hamster IgG or with 3% BSA/PBS for 33D1 staining and stained with biotin-conjugated 33D1, HMD1-5, HMD4-2, HMJ1-29 or HMJ2-1. For detection, Catalyzed Signal Amplification System, peroxidase (Dako Cytomation, Carpinteria, CA, USA) or Tyramide Signal Amplification Kit (PerkinElmer, Walthmam, MA, USA) was used. For staining ER-TR7, CD31 or B220, sections were blocked with 10% normal goat serum and Alexa488-labeled goat anti-rat IgG (Molecular Probes, Carlsbad, CA, USA) was used as secondary antibody. For staining with FITC-labeled mAb to F4/80, sections were blocked with 10% normal rabbit serum and Alexa488-labeled rabbit anti-FITC (Molecular Probes) was used as secondary antibody. Images were acquired on a microscope (Eclipse E800M; Nikon, Tokyo, Japan) equipped with a digital camera (DXM1200; Nikon) and processed using ACT-1 (Nikon). Fluorescent images were acquired on a microscope (Eclipse TE300; Nikon) equipped with a digital camera (C4742-98; Hamamatsu photonics, Hamamatsu, Japan) and processed using AquaCosmos (Hamamatsu photonics).

Results

Expression of Notch receptors and ligands on splenic DCs

We first examined the expression of Notch receptors and ligands on cell surface of splenic DCs. Flow cytometrical analysis defined 33D1 expression exclusively on the CD8⁻ DC subset (Fig. 1). Notch1, Notch2 and Notch3 were expressed at similar levels on both CD8⁻ and CD8⁺ subsets. In contrast, Notch4 was highly expressed on CD8⁺ DCs but not CD8⁻ DCs (Fig. 1). Expression of Notch ligands was also similar between CD8⁻ DCs and CD8⁺ DCs: Dll1 and Jagged2 were expressed at moderate levels and Jagged1 was expressed at a low level (Fig. 1).

Blocking of all Notch ligands, but not Dll1 alone, reduces CD8⁻ DCs in the spleen

To examine the role of Dll1 in the maintenance of CD8⁻ DCs, mice were treated with anti-Dll1-blocking mAb (HMD1-5) (12) on days 0 and 3, and the spleens were removed on day 7. As shown in Fig. 2(A), the blocking of Dll1 alone had little effect on the population of CD8⁻33D1⁺CD11c⁺ cells (CD8⁻ DCs) or CD8⁺33D1⁻CD11c⁺ cells (CD8⁺ DCs) in the spleen. No significant change was also observed on days 14 and 28 or with a high dose (1 mg) of HMD1-5 (data not shown). In addition, the percentage of CD8⁻ DCs in total splenocytes of Dll1 cKO mice (4) was not significantly reduced as compared with control mice (data not shown). Then, we additionally blocked Dll4, Jagged1 and Jagged2 by administrating a mixture of mAbs to these molecules (HMD4-2, HMJ1-29 and HMJ2-1, respectively). The combined blocking of Dll1, Dll4, Jagged1 and Jagged2 significantly reduced the CD8⁻ DC

compartment to a half of the control hamster IgG treatment ($P = 0.000096$), while the $CD8^+$ DC compartment was not affected (Fig. 2A). Immunohistochemical analysis showed a substantial decrease of $33D1^+$ cells in the splenic red pulp of the combination-treated mice (Fig. 2B).

Relative contribution of each Notch ligand to the maintenance of CD8⁻ DCs and MZ B cells

To address whether all these Notch ligands (Dll1, Dll4, Jagged1 and Jagged2) contribute to maintain $CD8^-$ DCs, one of these was excluded from the combined blockade. Blocking of Dll4, Jagged1 and Jagged2 did not reduce $CD8^-$ DCs significantly, while other blocking combinations of three Notch ligands reduced them significantly, suggesting the importance of Dll1 for the maintenance of $CD8^-$ DC subset (Fig. 3). Moreover, combinational blockade of Dll1 with Dll4, Jagged1 or Jagged2 also decreased $CD8^-$ DCs though blocking of any single Notch ligand did not (Fig. 3). These results suggest that Dll1 could be important but not only Dll1 but also Dll4, Jagged1 and Jagged2 contribute to the maintenance of $CD8^-$ DCs. On the other hand, MZ B cells were decreased exclusively by blockade of Dll1 but not the other Notch ligands (Fig. 3). Notably, the changes of total DCs ($CD11c^+$) in the spleen reflected those of $CD8^-$ DCs, while the $CD8^+$ DC compartment was not affected by any of the indicated treatments (Fig. 3).

Kinetics of splenic CD8⁻ DC reduction

It has been shown that Notch signal-deficient $CD8^-$ DCs exhibited increase of apoptosis in the spleen and suggested that Notch signals were required for their survival (3). Actually, the treatment with a mixture of antibodies against all Notch ligands (HMD1-5, HMD4-2, HMJ1-29 and HMJ2-1) reduced splenic $CD8^-$ DCs to half of the control treatment in 1.5 days (Fig. 4). Similar reduction was observed at day 3 while it was restored at day7 (Fig. 4). In contrast, Notch signaling was essential for the development of MZ B cells (12) and no significant decrease of MZ B cells was detected at day 1.5 (Fig. 4). Notably, Annexin V-positive apoptotic $CD8^-$ DCs were increased in mice blocked all Notch ligands (3.03 ± 0.079% versus 2.37 ± 0.17% hamster IgG control mice, $P = 0.0097$).

CD8⁻ DC reduction is associated with decrease of IL-12 secretion from splenic DCs

To determine whether this decrease of $CD8^-$ DCs by blocking of Notch ligands was related to functional reduction, DC cytokine responses to toll-like receptors (TLR) activation was analyzed. Stimulation of splenocytes with TLR7 agonist, imiquimod or R848 or TLR4 agonist LPS induced IL-12 secretion from $CD8^-$ DCs *in vitro* (Fig. 5). IL-12-secreting $CD8^-$ DCs induced by these TLR agonists were decreased in splenocytes from mice treated with a mixture of antibodies against Notch ligands (HMD1-5, HMD4-2, HMJ1-29 and HMJ2-1) while IL-12-secreting $CD8^+$ DCs were unchanged (Fig. 5).

Localization of Notch ligands in the spleen

Finally, the location of Dll1, Dll4, Jagged1 and Jagged2 in the spleen was determined. Immunohistochemical analysis demonstrated that all these Notch ligands were expressed primarily in

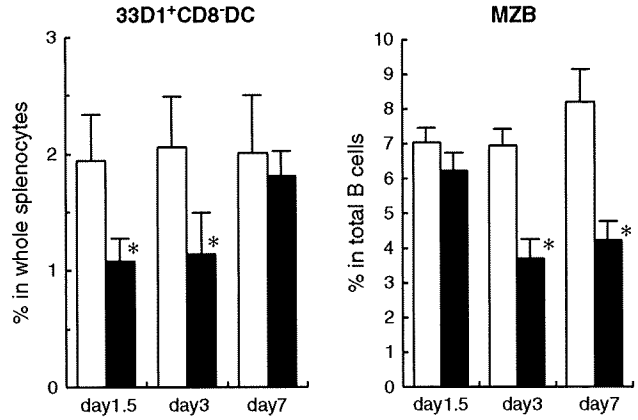

Fig. 4. Time course of $CD8^-$ DC reduction. Mice were treated with control hamster IgG (open columns) or a mixture of mAbs (HMD1-5, HMD4-2, HMJ1-29 and HMJ2-1; closed columns) once. Spleen cells were analyzed on indicated days. The percentages of $CD11c^{high}$/$33D1^+$/$CD8^-$ ($33D1^+CD8^-$ DC) among whole splenocytes and the percentage of MZ B cells ($B220^+$/$CD21^{hi}$/$CD23^{lo/-}$) among total B cells ($B220^+$) were analyzed by flow cytometry. Data are represented as the mean ± SD of three mice in each group. Similar results were obtained in two independent experiments. Data were analyzed statistically using unpaired Student's *t*-test. $*P < 0.05$ versus hamster IgG-treated control mice.

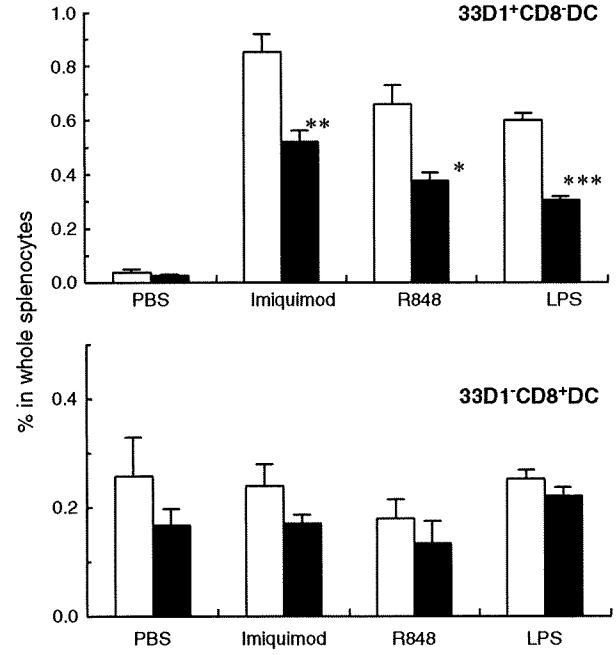

Fig. 5. Effects of anti-Notch ligand mAbs on IL-12 secretion from splenic DCs. Mice were treated with control hamster IgG (open columns) or a mixture of mAbs (HMD1-5, HMD4-2, HMJ1-29 and HMJ2-1; closed columns). Collagenase-treated splenocytes were cultured in the presence or absence of indicated TLR ligands. IL-12 production in DCs was detected by intracellular staining. The percentages of IL-12-secreting $CD11c^{high}$/$33D1^+$/$CD8^-$ ($33D1^+CD8^-$ DC) and $CD11c^{high}$/$33D1^-$/$CD8^+$ ($33D1^-CD8^+$ DC) cells among whole splenocytes were analyzed by flow cytometry. Data are represented as the mean ± SD of three mice in each group. Data were analyzed statistically using unpaired Student's *t*-test. $*P < 0.05$, $**P < 0.01$, $***P < 0.001$ versus hamster IgG-treated control mice.

the red pulp area where CD8⁻ DCs resided (Figs 2B and 6). ER-TR7⁺ reticular fibroblasts and F4/80⁺ macrophages localize mainly in the red pulp of the spleen. Accordingly, part of ER-TR7⁺ reticular fibroblasts expressed Dll1, Dll4, Jagged1 or Jagged2 (Fig. 6). Part of F4/80⁺ macrophages also expressed Dll1, Jagged1 or Jagged2 (Fig. 6). In addition, CD31⁺ vessels in the spleen expressed Dll1 or Jagged1 (Fig. 6). Though B cells were considered important in splenic DC homeostasis (13, 14), Notch ligands were not expressed on B cells (Fig. 6).

Discussion

Dll1 has been shown to be essential for the development of MZ B cells (4, 6). In this study, we found that Dll1 was also important for the maintenance of CD8⁻ DCs, but Dll4, Jagged1 and Jagged2 could also participate in this process. Indeed, a similar extent of CD8⁻ DC reduction was observed among Dll1-, Dll4-, Jagged1- and Jagged2-blocking mice and RBP-J CD11c-Cre⁺ cKO mice (3). Consistent with this notion, Jagged1 and Jagged2 were localized similar to Dll1. Therefore, it is likely that Jagged1 and Jagged2 as well as Dll1 could engage the Notch receptors on CD8⁻ DCs to maintain this population. CD8⁺ DCs are reported to reside in the white pulp area (9) where Notch ligands were not expressed, which may explain why this subset was not regulated by Notch signaling. The functional role of Notch4 uniquely expressed on CD8⁺ DCs will be determined in our future study.

Notch2 was essential for the development of MZ B cells and expressed higher on MZ B and precursors of MZ B cells than on T1 B and T2/Fo B cells (12). Cell surface expression of Notch receptors suggest that Notch1, Notch2 and Notch3 could be responsible for the Notch signaling to maintain CD8⁻ DCs in the spleen. The differential contribution of Jagged1 and Jagged2 to the homeostasis of CD8⁻ DCs and MZ B cells may be explained by their difference in the expression of Notch receptors. Indeed, the expression of Notch1 and Notch2 on CD8⁻ DCs was lower than that on

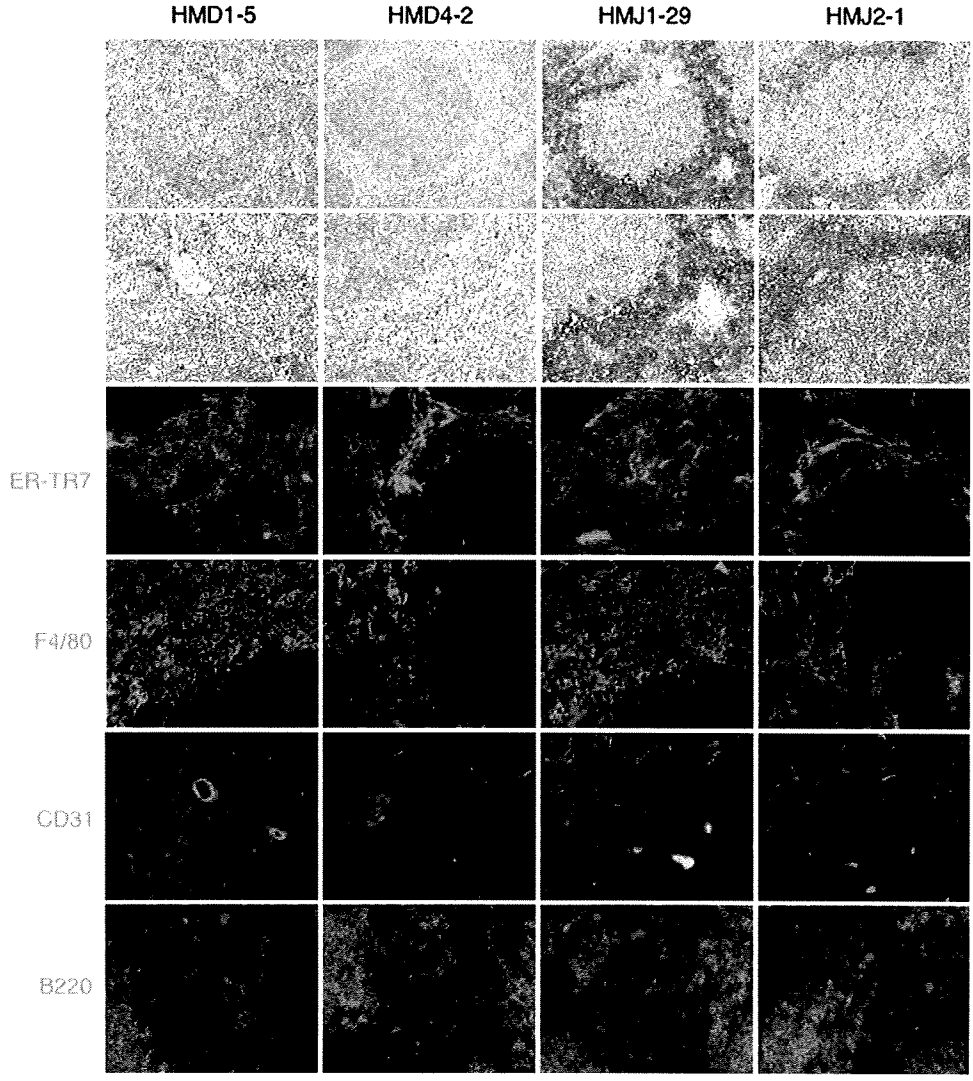

Fig. 6. Immunohistological analysis for localization of Notch ligands in the spleen. Spleen sections were stained with HMD1-5, HMD4-2, HMJ1-29 or HMJ2-1 (brown or red) and ER-TR7 or mAbs against F4/80, CD31 or B220 (green). Essentially, no staining was observed with control hamster IgG (not shown). Original magnification: top panels, ×100; the others, ×200.

B cells but Notch3 was expressed higher on CD8⁻ DCs (12). Thus, Notch3 may be a key Notch receptor to maintain CD8⁻ DCs via activation by Dll4, Jagged1 and Jagged2. Although Notch1 and Notch2 could be activated to maintain CD8⁻ DCs especially in a Notch3-deficient condition, it is intriguing to investigate whether CD8⁻ DCs are decreased in Notch3-deficient mice that are viable and fertile (15).

Splenic CD8⁻ DCs are short-lived. Parabiosis experiments have estimated that the half-life of splenic CD8⁻ DCs was ~7 days (16). Inhibition of Notch ligands decreased splenic CD8⁻ DCs earlier than its half-life at almost maximum level (1.5 days after mAbs treatment) in association with increased apoptosis of CD8⁻ DCs and it restored quickly (at day 7). A recent study using DC-specific RBP-J KO mice has determined increased apoptosis of CD8⁻ DCs in the spleen (3). These data indicate that Notch signaling contributes to survival of splenic CD8⁻ DCs. Functional significance of CD8⁻ DC reduction with the lack of Notch signaling has been demonstrated by the decrease of DC-mediated cytokine responses when injected with the TLR7 agonist imiquimod, which preferentially activates CD8⁻ DCs (3). Blocking of Notch ligands also reduced TLR agonists-induced IL-12 secretion from CD8⁻ DCs. MZ B cells are known to play roles in response to blood-borne pathogens and also in immune responses (17). Reduced MZ B cells through a defect of Notch signaling conferred high sensitivity to blood-borne bacteria, *Staphlococcus aures*, though it showed no obvious deficiency in the immune responses to thymus-dependent, thymus-independent type 1 and type 2 antigens (18).

Fringes are glycosyltransferases that modify the extracellular domain of Notch, enhancing its activation by Delta and inhibiting its activation by Jagged (19, 20). Therefore, the expression of Fringes in CD8⁻ DCs may be different from that in MZ B cells, leading to the differential contribution of Delta and Jagged Notch ligands. Further studies are needed to address these possibilities.

Funding

Grants-In-Aid from the Ministry of Education, Culture, Sports, Science and Technology, Japan (17016071).

Abbreviations

cKO	conditional knockout
Dll	Delta-like
DC	dendritic cell
ER	endoplasmic reticulum
MZ	marginal zone
TLR	toll-like receptors

References

1 Artavanis-Tsakonas, S., Rand, M. D. and Lake, R. J. 1999. Notch signaling: cell fate control and signal integration in development. *Science* 284:770.
2 Radtke, F., Wilson, A., Mancini, S. J. and MacDonald, H. R. 2004. Notch regulation of lymphocyte development and function. *Nat. Immunol.* 5:247.
3 Caton, M. L., Smith-Raska, M. R. and Reizis, B. 2007. Notch-RBP-J signaling controls the homeostasis of CD8- dendritic cells in the spleen. *J. Exp. Med.* 204:1653.
4 Hozumi, K., Negishi, N., Suzuki, D. *et al.* 2004. Delta-like 1 is necessary for the generation of marginal zone B cells but not T cells *in vivo*. *Nat. Immunol.* 5:638.
5 Kuroda, K., Han, H., Tani, S. *et al.* 2003. Regulation of marginal zone B cell development by MINT, a suppressor of Notch/RBP-J signaling pathway. *Immunity* 18:301.
6 Saito, T., Chiba, S., Ichikawa, M. *et al.* 2003. Notch2 is preferentially expressed in mature B cells and indispensable for marginal zone B lineage development. *Immunity* 18:675.
7 Steinman, R. M. 2003. Some interfaces of dendritic cell biology. *APMIS.* 111:675.
8 Shortman, K. and Liu, Y. J. 2002. Mouse and human dendritic cell subtypes. *Nat. Rev. Immunol.* 2:151.
9 Dudziak, D., Kamphorst, A. O., Heidkamp, G. F. *et al.* 2007. Differential antigen processing by dendritic cell subsets *in vivo*. *Science* 315:107.
10 Cheng, P., Nefedova, Y., Corzo, C. A. and Gabrilovich, D. I. 2007. Regulation of dendritic-cell differentiation by bone marrow stroma via different Notch ligands. *Blood* 109:507.
11 Elyaman, W., Bradshaw, E. M., Wang, Y. *et al.* 2007. JAGGED1 and delta1 differentially regulate the outcome of experimental autoimmune encephalomyelitis. *J. Immunol.* 179:5990.
12 Moriyama, Y., Sekine, C., Koyanagi, A. *et al.* 2008. Delta-like1 is essential for the maintenance of marginal zone B cells but not in the autoimmune mice. *Int. Immunol.* 20:763.
13 Kabashima, K., Banks, T. A., Ansel, K. M., Lu, T. T., Ware, C. F. and Cyster, J. G. 2005. Intrinsic lymphotoxin-beta receptor requirement for homeostasis of lymphoid tissue dendritic cells. *Immunity* 22:439.
14 Ngo, V. N., Cornall, R. J. and Cyster, J. G. 2001. Splenic T zone development is B cell dependent. *J. Exp. Med.* 194:1649.
15 Krebs, L. T., Xue, Y., Norton, C. R. *et al.* 2003. Characterization of Notch3-deficient mice: normal embryonic development and absence of genetic interactions with a Notch1 mutation. *Genesis* 37:139.
16 Liu, K., Waskow, C., Liu, X., Yao, K., Hoh, J. and Nussenzweig, M. 2007. Origin of dendritic cells in peripheral lymphoid organs of mice. *Nat. Immunol.* 8:578.
17 Pillai, S., Cariappa, A. and Moran, S. T. 2005. Marginal zone B cells. *Annu. Rev. Immunol.* 23:161.
18 Tanigaki, K., Han, H., Yamamoto, N. *et al.* 2002. Notch-RBP-J signaling is involved in cell fate determination of marginal zone B cells. *Nat. Immunol.* 3:443.
19 Bray, S. J. 2006. Notch signalling: a simple pathway becomes complex. *Nat. Rev. Mol. Cell Biol.* 7:678.
20 Visan, I., Yuan, J. S., Tan, J. B., Cretegny, K. and Guidos, C. J. 2006. Regulation of intrathymic T-cell development by Lunatic Fringe–Notch1 interactions. *Immunol. Rev.* 209:76.

ELSEVIER

Experimental Hematology

Experimental Hematology 2009;37:1318–1329

Development of monoclonal antibodies for analyzing immune and hematopoietic systems of common marmoset

Yoshie Kametani[a], Daisuke Suzuki[a], Kazuyoshi Kohu[b], Masanobu Satake[b], Hiroshi Suemizu[c], Erika Sasaki[c], Toshio Ito[c], Norikazu Tamaoki[c], Tomoko Mizushima[c], Manabu Ozawa[d], Kenzaburo Tani[e], Mitsuaki Kito[f], Hideo Arai[f], Akemi Koyanagi[g], Hideo Yagita[g,h], and Sonoko Habu[a,g,h]

[a]*Department of Immunology, Tokai University School of Medicine, Isehara, Japan;* [b]*Department of Molecular Immunology, Institute of Development, Aging Cancer, Tohoku University, Sendai, Japan;* [c]*Central Institute for Experimental Animals, Kawasaki, Japan;* [d]*Department of Molecular Therapy, Institute of Medical Science, Tokyo University, Tokyo, Japan;* [e]*Department of Molecular Genetics, Division of Molecular and Clinical Genetics, Medical Institute of Bioregulation, Kyushu University, Fukuoka, Japan;* [f]*DG RP Unit, Bioscience Department, Bioindustry Division, Oriental Yeast Co., Ltd., Tokyo, Japan;* [g]*Laboratory of Cell Biology;* [h]*Department of Immunology, Juntendo University School of Medicine, Tokyo, Japan*

(Received 6 June 2009; revised 19 August 2009; accepted 20 August 2009)

Objective. **Common marmosets are considered experimental animals of primates useful for medical research. We developed several monoclonal antibodies (mAbs) directed to CD molecules to gain initial insight into the immune and hematopoietic systems of this organism, and analyzed the basic cellularity and characters of marmoset lymphocytes.**

Materials and Methods. **Anti-marmoset CD antigen mAbs were prepared using marmoset antigen-expressing transfectants and used for flow cytometric analyses and cell fractionation. Expression of T-cell–related cytokine gene transcripts was examined in response to T-cell receptor stimulation by reverse transcription polymerase chain reaction analyses. Hematopoietic progenitor activities of marmoset bone marrow cells were examined in fractionated cells by mAbs against CD117 (c-kit) and CD34.**

Results. **CD4 and CD8 expression profiles in T-cell subsets of marmoset were essentially similar to those in mouse and human. $CD4^+$ and $CD8^+$ subsets were isolated from marmoset spleens. Detected transcripts after stimulation of T cells included Th1-, Th2-, and Th17-related cytokines in $CD4^+$ cells and cytotoxic proteases in $CD8^+$ cells, respectively. Colony-forming abilities were detected mainly in CD117 $(c\text{-kit})^+$ cells, irrespective of CD34 expression.**

Conclusions. **Marmoset immune system was basically similar to human and mouse systems.** **© 2009 ISEH - Society for Hematology and Stem Cells. Published by Elsevier Inc.**

Mice are the most commonly used experimental animals as an alternative for humans, and many disease models have been generated using these animals. However, because of the evolutional distance between the two species, there are remarkable differences recognized in their genetic and physiological functions [1–5]. In particular, humans and mice exhibit differences in various aspects of immunity, such as T-cell subset differentiation and cytokine signal transduction. For example, for Th17 differentiation, both interleukin (IL)-1 and IL-6 are necessary in humans, whereas transforming growth factor–β (TGF-β) and IL-6 are important in mice. Thus, mice are not always versatile as a human alternative, despite their ease in gene manipulation.

One of the approaches for overcoming this species specificity is to establish a human immune system in immunodeficient mice. For generating such humanized mice, severe combine immunodeficient (SCID), nonobese diabetic (NOD)-SCID, RAG2-null, and NOD/shi-SCID/IL-$2Rg^{null}$ (NOG) mice have been used as recipients because they each lack their own immunity, to varying degrees, because of gene mutation/deficiency [6–8]. On the other hand, human cord blood cells, lymphoid tissues/cells, or leukemic cells have been engrafted as donors into such mice [9–11]. Reconstitution of the human immune system in mice has been successful to varying extents, depending on both the type of recipient mouse and donor cells. In a combination

Offprint requests to: Sonoko Habu, M.D., Ph.D., Department of Immunology, Juntendo University School of Medicine, 2-1-1, Hongo, Bunkyo-ku, Tokyo 113-8421, Japan; E-mail: sonoko-h@med.juntendo.ac.jp

0301-472X/09 $–see front matter.
doi: 10.1016/j.exphem.2009.08.003

of human cord blood cells and NOG mice, T and B cells of human origin emerge in peripheral blood, but the produced antigen-specific human antibody is mainly immunoglobulin (Ig) M but not IgG [12–16]. This suggests that the interaction of T and B cells does not occur properly in these xenografted mice [17]. Thus, reconstitution of human immunity is not necessarily complete. Furthermore, use of human tissues may involve an ethical issue, precluding the possibility of preclinical use.

The common marmoset, a new world monkey, and humans are in the same evolutional entity of anthropoidea. The common marmoset is the only experimental animal among primates that has been artificially bred and maintained as a closed colony for >20 years. This species was identified as one of the most useful primates because of its size, availability, and widespread use in biomedical research [18,19]. Disease models of neurological disorders and human-specific virus infections have been established with this animal [20–24]. In particular, models of autoimmune diseases, such as experimental allergic encephalomyelitis, which resembles clinical and pathological features of human multiple sclerosis, compared to other animal models including other monkeys, have been generated and found to be useful for drug screening and evaluation [22,25,26]. Thus, compared to mice, common marmosets appear to emerge as a closer alternative to humans. Recently, we succeeded in the development of green fluorescent protein (GFP)–transgenic marmoset [27]. This might open another approach to human immunity in addition to the aforementioned human-to-mouse xenograft.

However, our knowledge of the immune system of the common marmoset is still not enough to establish it as an experimental animal and use as an alternative for human immunity and its disorders. One major obstacle to overcome initially is the lack of various fundamental molecular resources necessary for marmoset research. This led us to cloning and determining the primary structures of 30 of the most representative immune system–related genes of the marmoset [28]. In addition to the gene resources, antibodies directed toward immune-system–related molecules also have to be developed. Although anti-human antibodies have been screened for their cross-reactivity with marmoset immune cells, it is not certain whether cross-reacting antibodies, if any, authentically recognize the corresponding marmoset antigens [29,30].

In this study, we established several anti-marmoset monoclonal antibodies (mAbs) that were directed against CD4, CD8, CD25, CD45, and CD117 (c-kit). By using these mAbs, we have preliminarily characterized T-cell subsets and hematopoietic progenitors of the common marmoset, and we also analyzed expression profiles of various cytokine genes in T-cell subsets. The present findings are expected to serve as a basis for further development of the common marmoset as a useful experimental animal concerning primate immunology.

Materials and methods

Animals

Common marmosets were obtained through CLEA Japan (Tokyo, Japan) and kept at the Central Institute for Experimental Animals (Kawasaki, Japan) during the experiments. Experiments using common marmosets were approved by the Institutional Committee for Animal Care and Use and performed at Central Institute for Experimental Animals according to institutional guidelines. The marmoset age (1 to 4 years old) and sex were arbitrary. In some cases, marmosets were injected subcutaneously with 10 mg/kg/d of human granulocyte colony-stimulating factor (G-CSF; Neutrogin, Chugai Co. Ltd, Tokyo, Japan) for 5 successive days. Female 5- to 6-week-old BALB/c mice were purchased from Japan SLC (Hamamatsu, Japan) and kept in specific pathogen-free conditions in the animal facility at Juntendo University School of Medicine (Tokyo, Japan). NOD/Shi-scid, common gc-null (NOD/SCID/γc-null; NOG) mice were provided from the Central Institute for Experimental Animals (Kawasaki, Japan). Experiments using mice were performed following the guidelines set by the university.

Reverse transcription polymerase chain reaction, cDNA cloning, and sequence analyses

RNA was extracted from the cells using the RNeasy Mini Kit (Qiagen, Germantown, MD, USA). RNA at 50 ng was reverse-transcribed to cDNA and amplified using the primers and OneStep RT-PCR kit (Qiagen). Reverse transcription polymerase chain reaction (RT-PCR) amplification was performed under the following conditions: reverse transcription was at 50°C for 30 minutes, polymerase activation was at 95°C for 15 minutes with 33 cycles of PCR, each cycle consisting of denaturation at 94°C for 1 minute, annealing at 60°C for 1 minute, and extension at 72°C for 1 minute. PCR products were subjected to agarose gel electrophoresis. Primers used for PCR were as follows: for *IL-2*, 5′-ATGTACAGCATGCAGCTC GC-3′ and 5′-GCTTTGACAGAAGGCTATCC-3′; for *IL-4*, 5′-TGTCCACGGACACAAGTGCGA-3′ and 5′-CATGATCGTCTTT AGCCTTTCC-3′; for *IL-5*, 5′-GCCAAAGGCAAACGCAGAACG TTTCAGAGC-3′ and 5′-AATCTTTGGCTGCAACAAACCAGTT TAGTC-3′; for *IL-6*, 5′-ATGAACTCCTTCTCCACAAGCGC-3′ and 5′-GAAGAGCCCTCAGGCTGGACTG-3′; for *IL-10*, 5′-GGT TACCTGGGTTGCCAAGCCT-3′ and 5′-CTTCTATGTAGTTGA TGAAGATGTC-3′; for *IL-17A*, 5′-CTCCTGGGAAGACCTCAT TG-3′ and 5′-CAGACGGATATCTCTCAGGG-3′; for *IL-17F*, 5′-CA AAGCAAGCATCCAGCGCA-3′ and 5′-CATTGGGCCTGTACAA CTTCTG-3′; for *IFN-γ*, 5′-CTGTTACTGCCAGGACCCAT-3′ and 5′-CGTCTGACTCCTTCTTCGCTT-3′; for *TGF-β*, 5′-GCCCTG GACACCAACTACTGC-3′ and 5′-GTCGCATTTGCAGGAGCGC AC-3′; for *TNF-α*, 5′-GAGTGACAAGCCTGTAGCCCATGTT GTAGCA-3′ and 5′-GCAATGATCCCAAAGTAGACCTGCCCAG ACT-3′; for *granzyme B*, 5′-ATATGAGGCCAAGCCCCACT-3′ and 5′-TCTCCAGCTGCAGTAGCATA-3′; for *perforin-1*, 5′-GGCC TGTGAGGAGAAGAAA-3′ and 5′-GCCCATCAGGTACTGAC TCA-3′; for *HPRT*, 5′-TGACCAGTCAACAGGGGAC-3′ and 5′-GC TCTACTAAGCAGATGGC-3′. The procedure of cDNA cloning was the same as reported by us previously [28]. The primers used were as follows: for *granzyme B*, 5′-CCAAGAGCTAAAAGAGAGTAAG GGGGAAAC-3′ and 5′-AGCGGGGGCTTAGTTTGCTTCCTGTA GTTA-3′; for *perforin 1*, 5′-GTGTAGCCGCTTCTCTATACGGGA

TTCCAG-3′ and 5′-TTCAGTCCAAGCATACTGGTCCTTTC-CAAG-3′.

The tool for sequence homology search was BLAST [31], whereas that for multiple sequence alignment was CLUSTALW.

Construction of cDNA expression vectors

cDNA sequences of marmoset genes used in this study were based on AF452616 as *CD4*, DQ189217 as *CD8a*, DQ520834 as *CD25*, AB097501 as *CD34*, and AB097502 as *CD117*. RNA was extracted from cells by Isogen (Nippon Gene Co. Ltd., Tokyo, Japan) and reverse-transcribed to cDNA by Superscript (Invitrogen, Carlsbad, CA, USA). A portion of cDNA sequence corresponding to an extracellular domain of the protein was amplified by a PCR method, using cDNA as a template and AccuPrime Pfx DNA Polymerase (Invitrogen, Tokyo, Japan). The set of forward and reverse primers used were as follows: for *IL-2*, 5′-ATGTACAG-CATGCAGCTCGC-3′ and 5′-GCTTTGACAGAAGGCTATCC-3′; for *CD4*, 5′-CCACCATGAATGGGGGAATCCCTTTC-3′ and 5′-CACCGGGGGAGACCATGTGGGCA-3′; for *CD8α*, 5′-CCAC CATGGCCTCGCCAGTGACCGC-3′ and 5′-ACAGGCGAAGT CCAGCCCC-3′; for *CD25*, 5′-CCACCATGGATTCACAACTG CTGATG-3′ and 5′-CTTCGTCGTAAGTATGAATGTCTCC-3′; for *CD34*, 5′-ATGCTGGTCCGCAGGGGC-3′ and 5′-TCGGGAA TAACTCTGGTGGCTTGC-3′; for *CD45*, 5′-CCACCATG-TATTTGTGGCTTAAACTGCT-3′ and 5′-TGATTGAAATTTAC-TAACTGGGTG-3′; for *CD117*, 5′-CCACCATGAGA GGCGCTCGTGGCG-3′ and 5′-GAACAGGGTGTGGGGCTG-GATTTGC-3′. Each PCR product was inserted into the *EcoR*V site of pCXGFP-1 vector (GenBank, Accession No. AB281497) in order to express an extracellular domain of interest as a fusion protein with an enhanced EGFP.

Preparation of cDNA-transfected cells

pCXGFP-1 vectors expressing marmoset cDNAs were transfected into Chinese hamster ovary (CHO) cells by electroporation using Gene Pulser (BioRad, Tokyo, Japan) according to manufacturer's instructions. After G418 selection at 1 mg/mL, the GFP^+ cells were isolated by fluorescence-activated cell sorter.

Production of mAbs

We adopted the hydrodynamic immunization procedure reported by Song et al. [32]. Briefly, 25 mg pCX-GFP plasmid DNA was suspended in 2 mL saline and injected intravenously into BALB/c mice. Mice were immunized three to six times, and serum antibody titers were checked by flow cytometric analyses using cDNA-transfected cells as a source of antigen. Four days after a final boost, mice were sacrificed and splenocytes were fused with the mouse myeloma cell line P3U1 according to a standard procedure. Positive clones were identified by flow cytometry, isolated, expanded, and stocked.

Preparation of human blood cells

Human umbilical cord blood was obtained from full-term healthy newborns immediately after vaginal delivery. Informed consent was obtained from individual mothers according to the institutional guidelines, and the work was approved by the Tokai University Human Research Committee. Peripheral blood was collected from healthy human volunteers. Mononuclear cells were isolated from cord and peripheral blood by Ficoll-Paque (GE Healthcare Biosciences, Uppsala, Sweden) gradient centrifugation as reported previously [15].

Preparation and stimulation of marmoset lymphocytes

Thymi, intestinal lymph modes, or spleens were taken from marmosets and cells were released from the tissues. After red blood cells were lysed osmotically, cells were suspended in RPMI-1640 medium containing 10% fetal calf serum. Peripheral blood or bone marrow cells were collected from marmosets with heparin and centrifuged on Lymphocepal (IBL Co., Takasaki, Japan) at 2,000 rpm for 30 minutes. Mononuclear cells were collected and the remaining erythrocytes were lysed.

To stimulate T cells, the cells were cultured in medium supplemented with anti-human CD3 (SP34-2; BD Pharmingen, San Diego, CA, USA) and anti-human CD28 (CD28.2; eBioscience, San Diego, CA, USA) or TSST-1 (1 mg/mL; Toxin Tec. Co., Sarasota, FL, USA) for 24 hours. Then, the cells were harvested, incubated with anti-marmoset CD4 or CD8 mAb (prepared in this study) or anti-human CD20 mAb (B-Ly1, Dako, Glostrup, Denmark) at 4°C for 15 minutes, washed, and reincubated with anti-mouse IgG–magnetic cell sorting (MACS) micro beads for 15 minutes. After a final wash, CD4-, CD8- or CD20-positive cells were purified using a MACS system (Miltenyi Biotec, Gladbach, Germany).

Colony-forming assay using bone marrow–derived mononuclear cells

Cells were recovered from bone marrow of the common marmoset, and a mononuclear fraction was isolated using Lymphoprep (Axis-Shield, Oslo, Norway). Then cells were sorted into $CD34^+CD117^+$, $CD34^+CD117^-$, $CD34^-CD117^+$, and $CD34^-CD117^-$ fractions using FACS Aria (Becton Dickinson, Franklin Lakes, NJ, USA). Anti-marmoset CD34 mAb was reported previously [29], and anti-marmoset CD117 mAb was prepared in the present study. The sorted cells in each group were plated at 2×10^2 cells in 1 mL methylcellulose-containing medium (Methocult GF+ H4435; Stem Cell Technologies, Vancouver, Canada) in a 35-mm dish with human stem cell factor (SCF) (10 ng/mL), IL-3 (10 ng/mL), human erythropoietin (Epo) (2 U/mL), and human G-CSF (10 ng/mL) and cultured at 37°C in a 5% CO_2 atmosphere. After 14 days of culture, types and numbers of hematopoietic colonies (colony-forming units [CFU]) were counted according to standard criteria. Samples from one animal were processed for the assay in triplicate, and two different animals were used (experiments 1 and 2).

Transplantation of hematopoietic progenitors into NOG mice

$CD34^+CD117^+$ and $CD34^-CD117^+$ cells were purified from bone marrow of the common marmoset by cell sorter as described here. Purity was >98% according to flow cytometry. Nine-week-old NOG mice were irradiated with 2.5 Gy x-ray prior to transplantation, and the marmoset cells (6.7×10^5 for $CD34^+CD117^+$ cells/ 1.3×10^6 for $CD34^-CD117^+$ cells) were transplanted intravenously. Four weeks after transplantation, peripheral blood was collected via orbit under inhalation anesthesia. Mononuclear cells were prepared and reconstitution efficiency was calculated by the ratio of marmoset $CD45^+$ cells.

Flow cytometric analysis

Cells were incubated with labeled primary mAb for 15 minutes at 4°C and washed with 1% (w/v) bovine serum albumin-containing phosphate-buffered saline. In some cases, cells were reincubated with labeled secondary antibody. The flow cytometer was FACSCalibur

(Becton Dickinson). The mAbs used were as follows: purchased from BD Pharmingen were anti-human CD3-peridinin chlorophyll Cy5.5 (PerCP) (SP34-2), anti-human CD4-allophycocyanin (APC) (SK3), anti-human CD8–fluorescein isothiocyanate (FITC) (HIT8a), anti-human CD20 (B-Ly1), anti-human CD25-phycoerythrin (PE) (M-A251), anti-human CD34 (581), anti-human CD45-APC (HI30), anti-human CD117-APC (YB5.B8), streptavidine-PE and streptavidine-APC. Purchased from eBioscience were anti-mouse CD4-APC (GK1.5), anti-mouse CD8-FITC (53.67), anti-mouse CD45.1-APC (30-F11), anti-mouse CD25-PE (PC61) and anti-mouse CD34 (RAM34). Anti-mouse CD117-APC (3C1) was from CALTAG Laboratories (Burlingame, CA, USA), and anti-mouse IgM-PE and anti-mouse IgG-PE were from Jackson ImmunoResearch Inc. (West Grove, PA, USA). We previously obtained anti-marmoset CD8 and CD45 mAbs by a different approach from that taken in this study [33]. These two mAbs were used as controls in the present study.

Results

cDNA expression systems and generation of mAbs

In the previous study, we cloned and sequenced 37 cDNA of immune-related genes obtained from marmoset spleen cells. Among them, we selected CD4, CD8, CD25, CD45, and CD117 as the targets to develop mAbs against marmoset proteins in this study. In humans and mice, CD4, CD8, and CD25 are representative surface molecules of T lymphocytes, CD117, and CD34 are hallmarks of hematopoietic progenitors, and CD45 represents a pan-leukocyte antigen.

To express a marmoset-derived cDNA, a pCXGFP1 vector was used (Fig. 1A). A cDNA portion encoding an extracellular domain of marmoset protein of interest to us was inserted into the *EcoR*V cloning site. From a recombinant, a marmoset cDNA was expressed as a fusion protein with the transmembrane domain of human MICA and cytoplasmically located enhanced GFP. Transcription was driven by CAG promoter. This recombinant was injected into mice as a DNA vaccine to sensitize the animals. In parallel, for the purpose of screening antibody production, a source of antigen was prepared by transfecting this expression plasmid into CHO cells. The cells expressing a fusion protein were selected by incubating the culture in the presence of G418. The plasmid harbored the neomycin-resistant gene.

By conventional experimental procedures, we could isolate the following six mAb clones (a subclass of Ig indicated). They were the clone Mar4-33 producing anti-CD4 mAb (IgG1), the clone Mar8-10 producing anti-CD8 mAb (IgG1), the clone Mar25-3 producing anti-CD25 mAb (IgG1), the clone Mar45-14 producing anti-CD45 mAb (IgG1), the clone MA24 producing anti-CD34 mAb (IgM), and the clone Mar117-22 producing anti-CD117 mAb (IgG1). Each mAb, including the previously described clone MA24, that produces anti-CD34 IgM mAb [29] was labeled with fluorochrome.

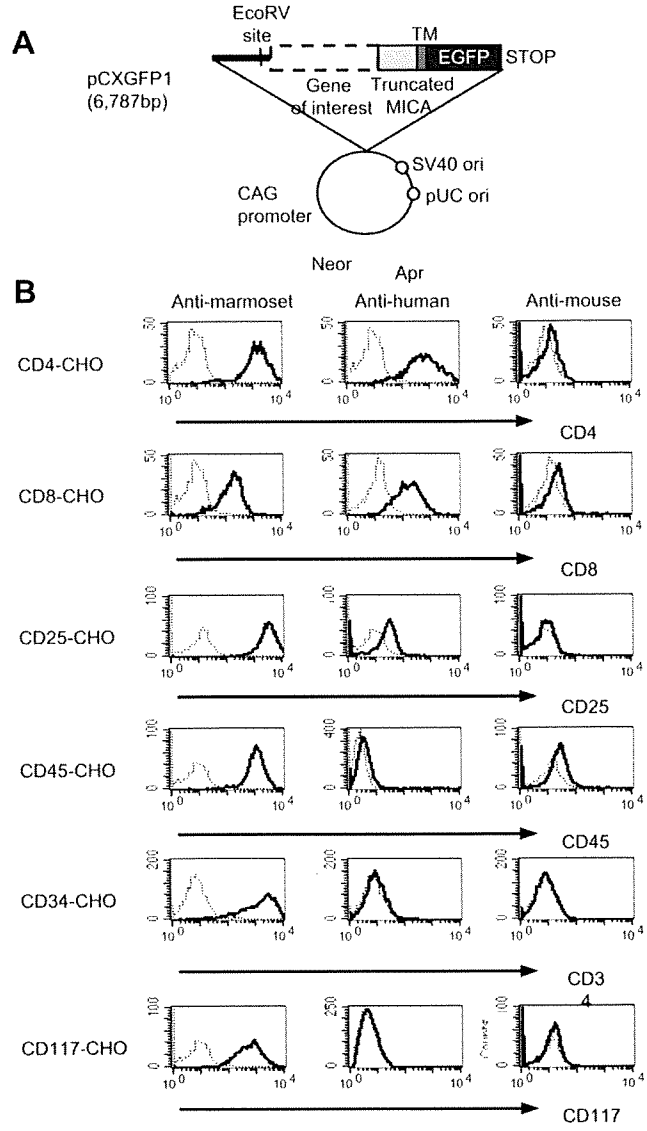

Figure 1. Reactivity of anti-marmoset, anti-human, and anti-mouse monoclonal antibodies (mAbs) against marmoset proteins expressed on CHO cells. (**A**) Schematic illustration of cDNA-expressing pCXGFP-1 vector. The *EcoR*V site is a cloning site of cDNA whose expression is driven by a CAG promoter. A gene of interest is expressed as a fusion protein with a transmembrane (TM) domain of human MICA and an intracytoplasmically located enhanced green fluorescent protein (EGFP) protein. The neomycin-resistance gene (Neor) is a drug selection marker. (**B**) Flow cytometric analyses of marmoset cDNA-expressing CHO cells stained by anti-marmoset, anti-human and anti-mouse mAbs.

Characterization of anti-marmoset mAbs

Figure 1B illustrates flow cytometric profiles of marmoset cDNA-transfected CHO cells stained by the newly prepared 6 mAbs and commercial mAbs. As can be seen in the left columns, each of the generated anti-marmoset mAb reacted with the respective antigen on CHO cells to a substantial degree of fluorescence intensity. This confirmed the authenticity of each mAb to recognize the respective antigen.

Cross-reactivity of anti-human mAb was examined in parallel (middle columns) using the cDNA-transfected CHO cells. An anti-human CD4 mAb (SK3) cross-reacted with marmoset CD4 as efficiently as anti-marmoset CD4 mAb. An anti-human CD8 mAb (HIT8α) gave a similar result. On the other hand, an anti-human CD25 mAb (M-A251) weakly cross-reacted with marmoset CD25, whereas anti-human CD45 (HI30), anti-human CD34 (581), and anti-human CD117 (YB5.B8) mAbs did not cross-react at all with the corresponding marmoset antigens. None of the anti-mouse mAbs showed any cross-reactivity with marmoset antigens (right columns).

Detection of marmoset T lymphocytes by anti-marmoset CD4 and CD8 mAbs

As shown in Figure 1B, the anti-marmoset mAbs reacted with the marmoset antigen that was overexpressed from transfected cDNA. Then, we investigated the reactivity of the same mAbs toward endogenously expressed marmoset antigens. As for the cells endogenously expressing these antigens, marmoset spleen cells were examined for reactivity of mAbs against marmoset CD4 and CD8 by two-color flow cytometric analysis. In the left panel of Figure 2A, marmoset splenocytes were stained by anti-marmoset CD4 and anti-human CD4 mAbs. The existence of double-positive cells in the upper right quadrant indicates the recognition of the same molecule by the two antibodies. A similar result was obtained when anti-marmoset CD8 and anti-human CD8 mAbs were used (see right panel of Fig. 2A).

CD3 is a pan-T lineage marker. We confirmed that an anti-human CD3ε mAb (SP34-2) recognized marmoset CD3ε-transfected cells (data not shown). In fact, marmoset splenocytes were stained with anti-human CD3ε and anti-marmoset CD4, or anti-human CD3ε and anti-marmoset CD8 mAbs, respectively (Fig. 2B). The $CD3\varepsilon^+$ T lymphocytes were divided into $CD4^+$ and $CD8^+$ cells. The combination of anti-human CD3ε and anti-human CD4 mAbs, or that of anti-human CD3ε and anti-human CD8 mAbs, gave the same result. It must be noted that anti-marmoset CD4 and anti-marmoset CD8 mAbs did not react with human peripheral blood mononuclear cells (Fig. 2C), indicating that anti-marmoset mAbs do not recognize the corresponding human antigens.

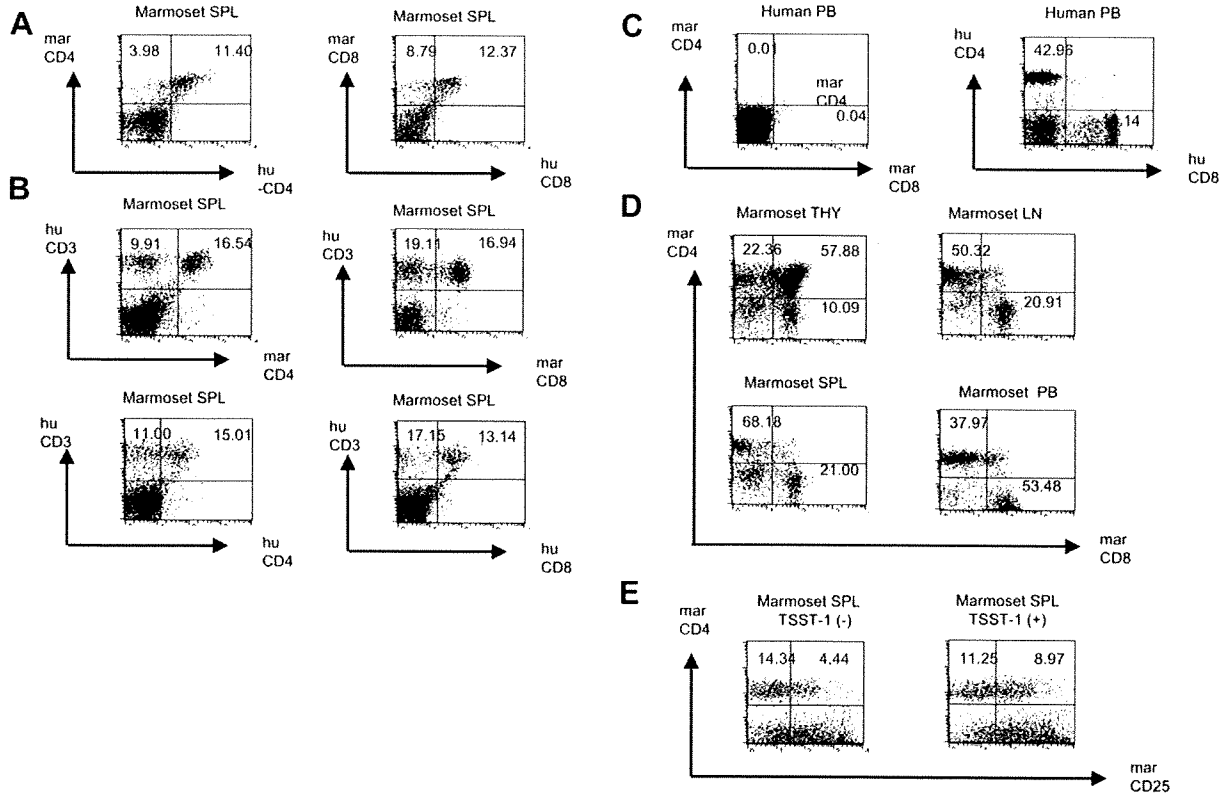

Figure 2. Characterization of anti-marmoset CD4, CD8, and CD25 monoclonal antibodies (mAbs), and identification of marmoset $CD4^+$ and $CD8^+$ T lymphocytes. (**A**, **B**) Marmoset splenocytes (SPL) were stained by the indicated mAbs, and their flow cytometric patterns are displayed. The mAbs used were anti-marmoset CD4, anti-marmoset CD8, anti-human CD4, anti-human CD8 and anti-human CD3ε. (**C**) Flow cytometry of human peripheral blood (PB) mononuclear cells. The mAbs were used as indicated. (**D**) Flow cytometry of marmoset-derived thymocytes (THY), SPL, lymph node cells (LN), and PB mononuclear cells. Anti-marmoset CD4 and CD8 mAbs were used as indicated. (**E**) Flow cytometry of marmoset SPL stained with anti-marmoset CD4 and anti-marmoset CD25 mAbs. Freshly isolated splenocytes (left) and the cells treated with TSST-1 in vitro (right) were analyzed.

Table 1. Comparison of Callithrix jacchus–derived CD34 and c-kit with human and mouse orthologs

Protein	Identical aa residues (%)		
	Marmoset vs human	Marmoset vs mouse	Human vs mouse
CD34	80	60	63
c-kit	94	81	82

Amino acid sequences of CD34 and c-kit from common marmoset (BAD04017.1 and BAD04018.1, respectively) were compared by BLAST homology search with human and mouse orthologs (human CD34, NP_001020280.1; human c-kit, NP_000213.1; mouse CD34, NP_598415.1; mouse c-kit, NP_066922.1) in three way pair-wise comparisons. The numbers indicate the percentages of identical aa residues between the two proteins compared.

These results confirmed that anti-marmoset CD4 and CD8 mAbs indeed recognize endogenous molecules. Then we also examined the distribution of T-cell subsets in other marmoset lymphoid tissues using these two mAbs (Fig. 2D). In marmoset thymi, the four subpopulations detected were $CD4^-CD8^-$, $CD4^+CD8^+$, $CD4^+CD8^-$, and $CD4^-CD8^+$, whereas only the two mature subsets $CD4^+CD8^-$ and $CD4^-CD8^+$ were detected in marmoset peripheral lymphoid tissues, such as spleen, lymph node, and peripheral blood. The profiles of these T-cell subsets were indistinguishable from those seen in human and mouse lymphoid tissues.

CD25 has been identified as an activation marker expressed on T cells in mice and humans. Then, mAb against marmoset CD25 was used to determine whether CD25 is expressed on marmoset splenocytes pre- and/or poststimulated with TSST-1 superantigen derived from *Staphylococcus aureus*, which can strongly stimulate $CD4^+$ T cells via T cell receptor (TCR)-β chain. The results showed an increase of CD25-expressing cells in $CD4^+$ cells (23–44%) after TSST-1 stimulation, indicating that CD25 is induced to express via T-cell activation in marmosets as well as in humans. A relative proportion of $CD25^+$ cells without CD4 expression in both pre– and post–TSST-1 stimulation was observed (Fig. 2E), and these $CD4^-CD25^+$ cells may belong to non–T cells, such as B cells and dendritic cells (DCs), as will be discussed later.

Cytokine gene expression profiles in marmoset T lymphocytes

Because the existence of $CD4^+$ and $CD8^+$ fractions was confirmed in lymphoid tissues, we then examined the cytokine expression profiles in marmoset T lymphocytes. To purify $CD4^+$ and $CD8^+$ cells from marmoset spleens, biotin-labeled anti-marmoset mAbs were used. As a control, B lymphocytes were isolated using anti-human CD20 mAb, because a transfectant expressing marmoset CD20 was recognized by anti-human CD20 (data not shown). The spleen cells were stimulated in vitro by anti-human CD3ε mAb, anti-human CD3ε, and anti-human CD28 mAbs, or superantigen TSST-1. After that, CD4 T cells were purified and RNA was prepared from the cells for semi-quantitative RT-PCR analyses (Fig. 3). Primers were designed based on published sequences of marmoset cDNAs.

In splenic $CD4^+$ cells (Fig. 3A), transcripts of *IL-4, IL-5, IL-6, IL-10, IL-17A, IL-17F,* and *IFN-γ* were barely or only slightly detected prior to stimulation, but were induced substantially by T-cell stimulation. *IL-2* induction was observed only after stimulation by TSST-1. In contrast, a relatively high amount of transcripts was detected for *TGF-β* and *TNF-α* prior to stimulation, and their expression persisted after stimulation. All of the $CD4^+$cells freshly isolated from five marmosets' peripheral blood showed a similar transcription profile to those in spleen cells (Fig. 3B).

$CD8^+$ splenic T cells were also examined (Fig. 3C). *IL-2* transcript was not detected before stimulation, but was substantially induced by TCR-mediated stimulations. Expression of *granzyme B* and *IFN-γ* was moderately

Table 2. Colony formation of marmoset bone marrow progenitor cells

Group[a]	CFU-mix[b]	CFU-G[b]	CFU-GM[b]	CFU-M[b]	Mega[b]	GFU-E/CFU-E[b]
Experiment 1						
$CD34^+/c\text{-}kit^+$	2 ± 1.4	6.3 ± 1.7	5.3 ± 1.9	0.3 ± 0.5	1 ± 1.4	2 ± 0.8
$CD34^+/c\text{-}kit^-$	0 ± 0	1.3 ± 0.5	0.7 ± 0.9	2 ± 0	1 ± 0	1 ± 0.8
$CD34^-/c\text{-}kit^+$	1.3 ± 0.5	5.3 ± 1.2	3.0 ± 0.8	0.3 ± 0.5	0 ± 0	4.0 ± 1.6
$CD34^-/c\text{-}kit^-$	0.7 ± 0.9	2 ± 0.8	1 ± 0.8	0 ± 0	1 ± 0	0.7 ± 0.9
Experiment 2						
$CD34^+/c\text{-}kit^+$	4.3 ± 2.1	12 ± 2.9	12 ± 1.6	1.7 ± 0.5	0.3 ± 5	6 ± 0.8
$CD34^+/c\text{-}kit^-$	0 ± 0	0.3 ± 0.5	0 ± 0	2 ± 0	0 ± 0	0 ± 0
$CD34^-/c\text{-}kit^+$	1.0 ± 0.8	8.7 ± 1.7	9.0 ± 3.7	5.0 ± 0	0.3 ± 0.5	6.7 ± 1.9
$CD34^-/c\text{-}kit^-$	0 ± 0	0.3 ± 0.5	0.7 ± 0.5	4 ± 1.4	0 ± 0	0 ± 0

Data are expressed as mean ± standard deviation.

[a]Marmoset bone marrow cells were sorted to four fractions according to CD34 and c-kit expressions and cultured in methylcellulose-containing medium for 2 weeks.

[b]Colony-forming unit (CFU)-mix, colony-forming unit granulocyte (CFU-G), colony-forming unit granulocyte-macrophage (CFU-GM), colony-forming unit macrophage (CFU-M), megakaryocyte (Mega)/colony-forming unit erythroid (GFU/CFU-E)/2 × 10^2 sorted bone marrow cells are shown. Colonies in triplicate were counted by microscopy. One marmoset per experiment was used.

detected before stimulation, and was significantly upregulated by stimulation. In contrast, *perforin-1* expression was sufficiently detected without stimulation and did not show any enhancement with stimulation.

Overall, the expression profiles of various cytokine genes seen in marmoset T cells were generally similar to those observed in humans and mice.

A primary structure of marmoset granzyme B gene

In the previously described plasmid construction and RT-PCR analyses, we utilized marmoset cDNA sequences that had mostly been reported in our previous study [28]. Exceptions were *perforin 1* and *granzyme B*. The nucleotide and deduced amino acid sequences of these two genes were newly determined in this study and were registered at National Center for Biotechnology Information (NCBI) as EU918127 and EU918128, respectively.

An interesting feature was observed in the primary sequence of *granzyme B* transcript (Fig. 4). Near the carboxy terminus of open reading flame, an additional sequence of 317 nt was inserted, which was not found in the corresponding region of human and chimpanzee *granzyme B* (see the sequence indicated by blue in (Fig. 4A), and note that Hs, Pt, and Cj represent human, chimpanzee and the common marmoset, respectively). This insertion caused a shift in the reading frame (see the location of termination codon indicated by red). Thus, the number of amino acid residues in the predicted marmoset polypeptide became longer by 23 aa at its carboxy terminus compared to human and chimpanzee granzyme B proteins (Fig. 4B). We cloned the genomic DNA from marmoset peripheral blood cells, and confirmed the insertion of the sequence in question into the exactly corresponding site of *granzyme B* gene (data not shown). Interestingly, the BLAST tool revealed a close homology of the inserted sequence to the

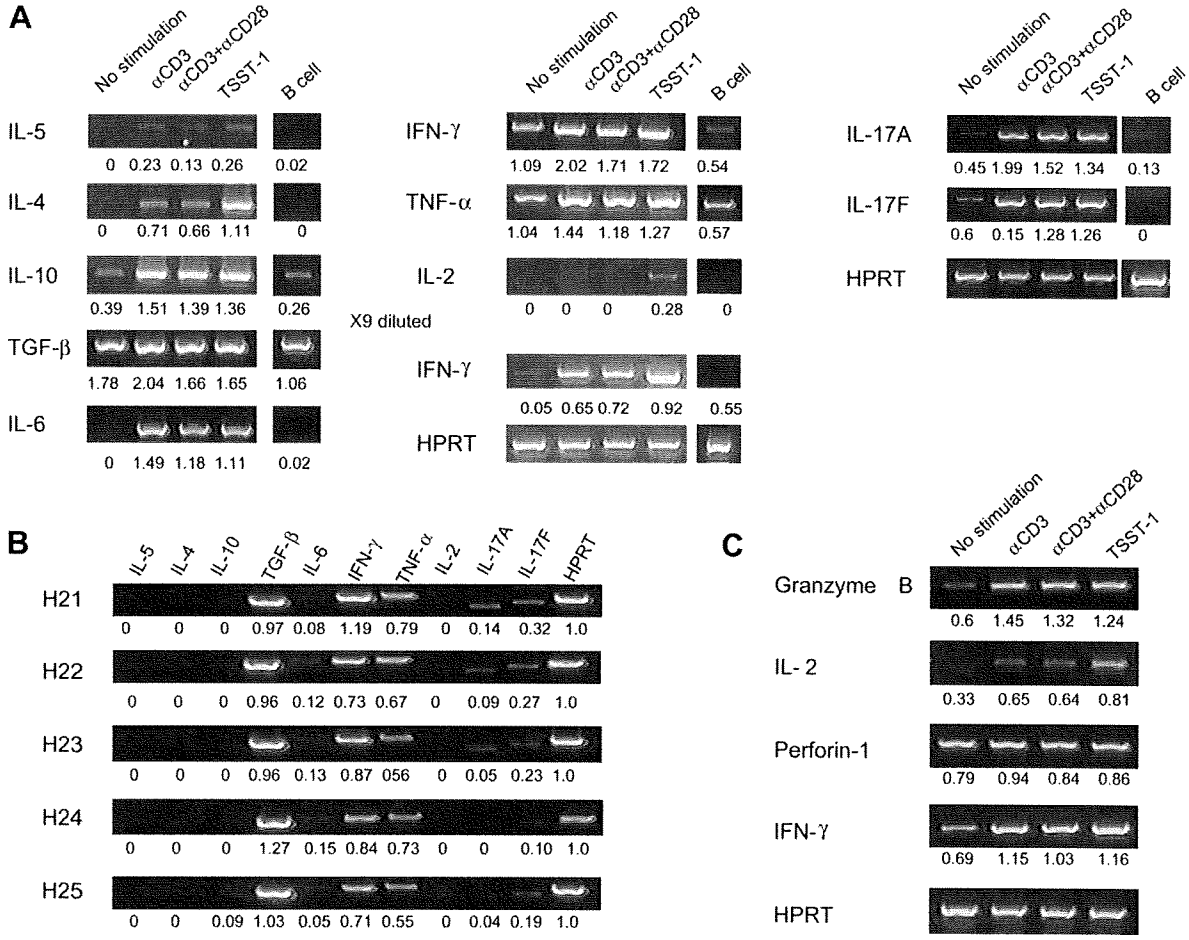

Figure 3. Semi-quantitative reverse transcriptase polymerase chain reaction (RT-PCR) analyses of marmoset cytokine gene transcripts. $CD4^+$ (**A**) and $CD8^+$ cells (**C**) were isolated from marmoset spleens and stimulated in vitro with anti-CD3, anti-CD3/anti-CD28 or TSST-1, respectively. $CD4^+$ cells were prepared from peripheral blood (PB) of normal marmosets (**B**). H21 to H25 represent individual marmoset numbers. RNA was prepared from the cells and processed for RT-PCR. B lymphocytes were isolated from marmoset spleens using anti-human CD20 monoclonal antibody (mAb), and its RNA was used in parallel. The amplified fragments were quantified and shown as indexes calculated using the formula (cytokine/HPRT). HPRT = hypoxanthine-guanine phosphoribosyltransferase; IFN = interferon; IL = interleukin; TGF = transforming growth factor; TNF = tumor necrosis factor.

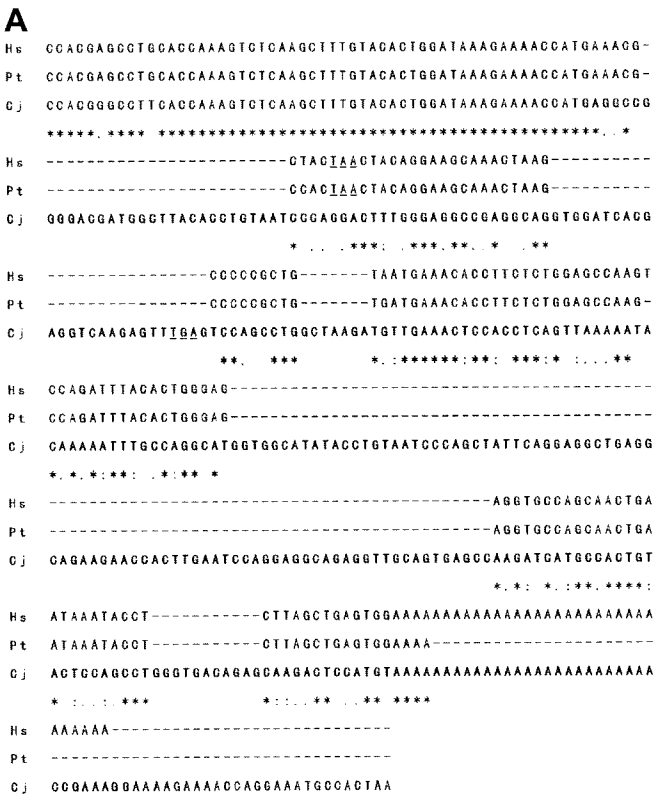

Figure 4. Insertion of *Alu*-like sequence into the marmoset *granzyme B* gene. (**A**) Alignment of *granzyme B* transcripts from human (Hs, NM_004131.3), chimpanzee (Pt, XM_509879.2) and common marmoset (Cj, EU918128.1). The 3′ portions of each transcript were aligned using the CLUSTALW tool. The common marmoset sequence indicated by bold, which does not have a counterpart in the transcripts from human and chimpanzee, is the Alu sequence. The termination codons of open reading flame (ORF) are indicated by underlines. Asterisks indicate identical residues. (**B**) Alignment of amino acid sequences of granzyme B proteins from human (NP_004122), chimpanzee (XP_509879), and common marmoset (EU918128). (**C**) Alignment of common marmoset-derived 317 nucleotide sequence (indicated by bold in panel **A**) with the human-derived *Alu-J* element.

human *Alu-J* element (Fig. 4C). Thus, the *Alu*-insertion into the ORF of *granzyme B* gene appears to be a feature unique to the common marmoset.

Detection of hematopoietic progenitor activity in marmoset bone marrow

CD117 and CD34 are the representative markers of murine and human hematopoietic progenitors, respectively. An extent of sequence conservation among the orthologous proteins of human, the common marmoset and mouse origin was examined by BLAST homology search (Table 1). The numbers therein represent the percentages of identical amino acid residues in three-way pair-wise comparisons. It can be seen that CD34 is relatively divergent among the three species, whereas CD117 is better conserved.

We then examined the activity of hematopoietic progenitors in marmoset bone marrow. Marrow cells were stained with anti-marmoset CD117 and CD34 mAbs (Fig. 5A). Four distinct fractions, namely $CD117^+CD34^+$, $CD117^+CD34^-$, $CD117^-CD34^+$, and $CD117^-CD34^-$, were detected. These anti-marmoset mAbs did not detect a positive population in human cord blood cells due to the lack of cross-reactivity with human antigens.

Using these mAbs, the four fractions described here were isolated from marmoset bone marrow cells by flow cytometry and assayed for their colony-forming activity in vitro. Human recombinant cytokines were added to the culture. Figure 5B shows the morphological appearance of burst-forming unit erythroid (BFU-E), colony-forming unit granulocyte (CFU-G), colony-forming unit macrophage (CFU-M), and colony-forming unit granulocyte-macrophage (CFU-GM) in the isolated $CD117^+CD34^+$ cells. At a level of microscopic resolution, these marmoset-derived colonies were indistinguishable from those of human and mouse. The

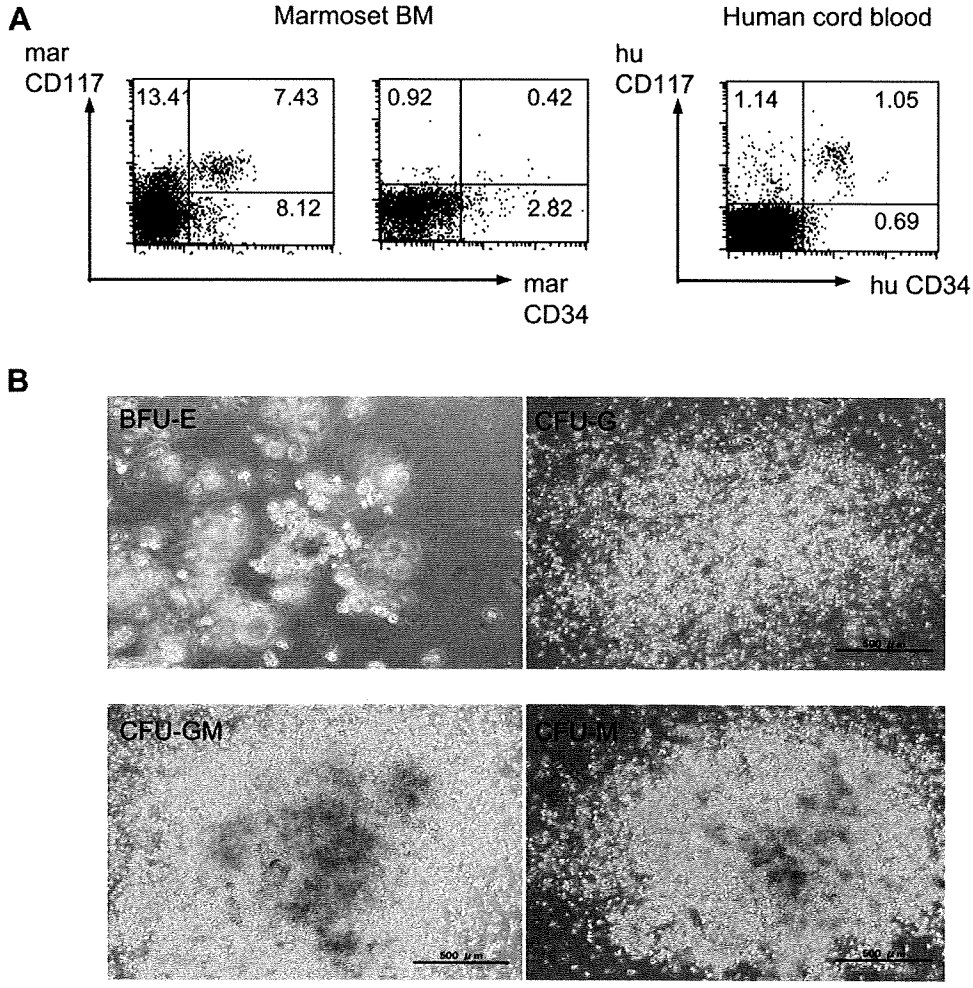

Figure 5. Hematopoietic progenitors in marmoset bone marrow as assayed in vitro. (**A**) Marmoset bone marrow (BM) cells and human cord blood cells were stained with the indicated monoclonal antibodies (mAbs), and their flow cytometrical patterns are displayed. The mAbs used were anti-marmoset CD117, anti-marmoset CD34, anti-human CD117, and anti-human CD34. (**B**) Morphological appearance of marmoset colonies formed in vitro. A $CD117^+CD34^+$ fraction was isolated from marmoset bone marrow, and assayed for colony-forming activity in the cytokine-supplemented culture. Phase contrast microscopic pictures are presented for burst-forming unit erythroid (BFU-E), colony-forming unit granulocyte (CFU-G), colony-forming unit macrophage (CFU-M), colony-forming unit granulocyte-macrophage (CFU-GM), respectively.

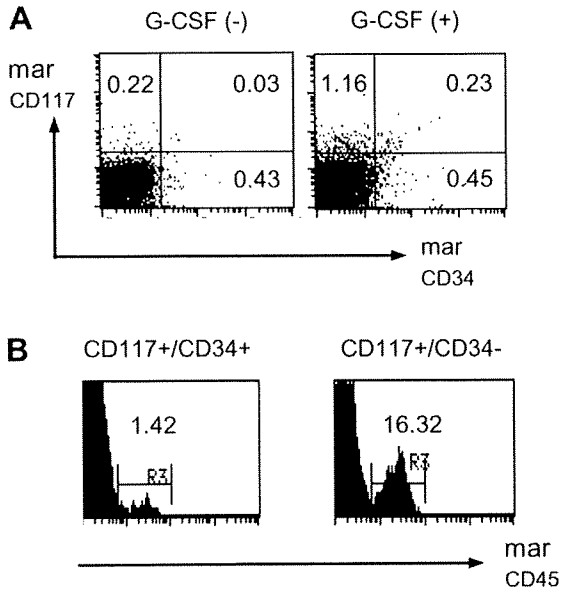

Figure 6. Hematopoietic progenitors in marmoset bone marrow as assayed in vivo. (**A**) Detection of peripherally mobilized progenitors in response to granulocyte colony-stimulating factor (G-CSF) injection. A marmoset individual was intravenously inoculated with human recombinant G-CSF, and peripheral blood was collected prior to (left panel) and 48 hours after the injection (right panel). Blood cells were stained using anti-marmoset CD117 and CD34 monoclonal antibodies (mAbs). (**B**) Lymphopoietic activity of marmoset progenitors as assayed in NOG mice. The $CD117^+CD34^+$ (left panel) and $CD117^+CD34^-$ (right panel) fractions isolated from marmoset bone marrow were inoculated into NOG mice, and 7 weeks after transplantation, peripheral blood was collected and stained using anti-marmoset CD45 mAb.

numbers of each colony were counted in each fraction and their average numbers are shown in Table 2. Quite similar numbers of colonies were formed from $CD117^+CD34^+$ and $CD117^+CD34^-$ fractions. However, only very weak colony-forming activity was detected for $CD117^-CD34^+$, and almost no activity for $CD117^-CD34^-$. This result suggests that hematopoietic activity as assayed in vitro resides mainly in the $CD117^+$ cells irrespective of CD34 expression.

Activity of marmoset hematopoietic progenitors as assayed in vivo

As described here, we could detect hematopoietic progenitors in marmoset bone marrow using marmoset-specific mAbs. Next, we examined the in vivo activity of marmoset progenitors. Human G-CSF was injected intravenously into marmosets. After 48 hours, peripheral blood was collected and stained with anti-marmoset mAbs (Fig. 6A). A $CD117^+$ fraction was not apparent in peripheral blood prior to G-CSF injection (left panel), but became evident after injection (right panel), corresponding to a sevenfold increase from 0.03% (left) to 0.23% (right). This indicates a mobilization of hematopoietic progenitors in response to G-CSF.

We also assayed the lymphopoietic activity of marmoset progenitors in vivo. For that, we used NOD/shi-SCID/IL-$2Rg^{null}$ (NOG) mice, a severe immunodeficient mouse cell line, because the mice have higher multipotential engraftment than any other mouse lines. The $CD117^+CD34^+$ and $CD117^+CD34^-$ fractions were isolated as mentioned here, and individually inoculated into NOG mice. After 7 weeks, peripheral blood was collected and stained for marmoset CD45 (Fig. 6B). In an individual inoculated with the $CD117^+CD34^-$ fraction, a substantial marmoset $CD45^+$ fraction emerged. In addition, the $CD20^+$ fraction was also observed in the $CD117^+CD34^-$-inoculated NOG mouse (data not shown). These observations indicate that the $CD117^+$ fraction developed into marmoset leukocytes, including a B-cell lineage, in vivo.

Discussion

In this study, to gain insight into how close or distant the immune system of the common marmoset is to that of humans and/or mice, we developed several mAbs directed toward marmoset antigens on T lymphocytes or on putative hematopoietic progenitors. CHO cells transfected with cDNAs and expressing marmoset proteins were initially used for screening the mAbs we produced against marmoset antigens. These cells were also used to examine the cross-reactivity of commercially available mAbs with human or mouse proteins. None of the examined anti-mouse mAbs showed any reactivity with marmoset antigens expressed on CHO cells, highlighting the great distance between marmoset and mouse epitopes. On the other hand, although mAbs against human CD34, CD45, and CD117 did not cross-react with respective marmoset antigens, other anti-human mAbs, including anti-CD4, anti-CD8, and anti-CD25 exhibited significant cross-reaction with the respective marmoset antigens. The reverse was not the case. The anti-marmoset CD4 or CD8 that we generated did not react with human CD4 or CD8. These observations suggest that use of anti-marmoset mAbs as was done in the present study would be ideal for examining marmoset immunity, although some anti-human mAbs could also be used as an alternative choice.

Marmoset $CD4^+$ T cells isolated from spleen cells and peripheral blood by using the established anti-marmoset mAbs showed various cytokine transcripts with TCR-mediated signaling. The induced cytokine transcripts included *IFN-γ*, *IL-4*, *IL-5*, *IL-10*, *IL-6*, and *IL-17*. These cytokines are produced from Th1, Th2, and Th17 T-cell subsets and play an important role in the immune response of humans and mice, suggesting that marmosets may have a similar immune function to humans. *TNF-α* and *TGF-β* transcripts were constitutively detected in marmoset $CD4^+$ cells even

prior to stimulation, which is not different from human and mouse. It must be emphasized that the present study established the authenticity of marmoset-derived cytokine transcripts because we designed the primers for PCR based on the marmoset sequences. On the other hand, the previous studies determined the marmoset cytokine transcripts by utilizing primers that were deduced by comparing the human and mouse orthologous genes [21,34]. Such an ambiguous method might allow the detection of only a few examples of cytokines.

TCR-stimulation caused an increment of *granzyme B* transcripts but not of *perforin 1* in these $CD8^+$ cells. In human, γδ T cells lose naïveness during childhood and start to express *perforin 1* constitutively [5,35]. Thus, one may speculate that the constitutive expression of *perforin 1* observed in the unstimulated marmoset $CD8^+$ T cells may not be detectable in resting cells but in already activated cells in some way. This is possible because the marmosets used were maintained under conventional, not pathogen-free, conditions. Alternatively, γδ T cells might be dominating in peripheral tissues of marmosets, which we could not yet determine as we have not cloned cDNA of any TCR chain genes, particularly γδ chains. Elucidation of this point requires development of anti-marmoset TCR γδ mAbs.

TSST-1 treatment of marmoset $CD4^+$ T cells enhanced their CD25 expression, reflecting the fact that CD25 expression is induced through the TCR-coupled activation process. To be noted is the existence of a $CD25^+$ subfraction in the freshly isolated splenic $CD4^-$ cells as well as $CD4^+$ T cells. The latter cells could be activated ones because they are maintained in non-specific pathogen free (SPF) environment as described here. Of a $CD4^-CD25^+$ fraction, they belong to non-T cells such as B cells and DCs, as shown in the past reports that these cells in human and mouse are induced to express CD25 if they are activated. In mouse and human, a $CD4^-CD25^+$ $CD20^+$ phenotype has been reported to represent B cells [36,37]. Further analyses of CD25 expression in marmoset resting B cells are required, particularly for developmental genetics/biology.

We generated and utilized anti-marmoset CD117 and CD34 mAbs for hematopoietic analysis. The percentage of $CD117^+CD34^+$ fraction was significantly increased in peripheral blood of marmosets receiving human G-CSF injection. These $CD117^+CD34^+$ cells exhibited multidifferentiating capabilities into myeloid and erythroid lineages by in vitro colony-forming assays. Furthermore, these double-positive cells, when transplanted into NOG mice, generated $CD45^+$ cells. Therefore, the $CD117^+CD34^+$ fraction most likely contains hematopoietic progenitor activity. The marmoset $CD34^+$ fraction reported to possess colony-forming activity [29] might have contained $CD117^+$ cells. In fact, as seen in Table 2, $CD117^+$ cells with and without CD34 expression showed higher hematopoietic activity than $CD117^-$ cells, while human $CD34^-CD117^+$ cells are reported to differentiate mainly to erythroid lineage cells [38]. A human $CD34^+$ fraction has been reported to possess progenitor activity into various cell lineages, including lymphocytes and DCs [39–41]. However, $CD34^+CD117^-$ cells are reported to possess less multipotentiality [41]. In mice, hematopoietic progenitor activity is present in $CD34^-CD117^+SCA\text{-}1^+$ cells [42,43]. Therefore, the previously known markers for hematopoietic progenitors may vary from species to species. The details of whether marmoset progenitors are more alike to mouse or human have to be investigated in greater detail.

In summary, the cell and cytokine profiles seen in marmoset helper and killer T cells were essentially reminiscent of those in human and mouse. Several marmoset antigens showed cross-reactivity with anti-human mAbs, suggesting a closer relationship of marmoset to human. The development of sophisticated analytical tools including mAbs should eventually contribute to the establishment of marmoset hematopoietic and immune systems as a human model.

Acknowledgments

We thank Dr. Hideki Kato, Hamamatsu Medical University (Shizuoka, Japan) for helpful discussions and for providing blood of common marmosets. We also thank Dr. Shuji Takabayashi, Fumika Toyota, and members of The Institute for Experimental Animals (Kanagawa, Japan) for help in collecting and shipping samples. This work was supported by a research grant from Japan Science Promotion (Tokyo, Japan) to S.H.

Conflict of Interest Disclosure

No financial interest/relationships with financial interest relating to the topic of this article have been declared.

References

1. Rautajoki K, Kylaniemi M, Raghav S, Rao K, Lahesmaa R. An insight into molecular mechanisms of human T helper cell differentiation. Ann Med. 2008;40:322–335.
2. Mestas J, Hughes C. Of mice and not men: differences between mouse and human immunology. J Immunol. 2004;172:2731–2738.
3. Shortman K, Liu Y-J. Mouse and human dendritic cell subtypes. Nat Rev Immunol. 2002;2:151–161.
4. Karaghiosoff M, Neubauer H, Lassnig C, et al. Partial impairment of cytokine responses in Tyk2-deficient mice. Immunity. 2000;13:549–560.
5. De Rosa S, Andrus J, Perfetto S, et al. Ontogeny of gd T cells in humans. J Immunol. 2004;172:1637–1645.
6. Martin A, Valentine M, Unger P, Yeung S, Shults L, Davies T. Engraftment of human lymphocytes and thyroid tissue into scid and rag2-deficient mice: absent progression of lymphocytic infiltration. J Clin Endocrinol Metabol. 1994;79:716–723.
7. Pflumio F, Izac B, Katz A, Shultz L, Vainchenker W, Coulombel L. Phenotype and function of human hematopoietic cells engrafting immune-deficient CB17-severe combined immunodeficiency mice and nonobese diabetic-severe combined immunodeficiency mice after transplantation of human cord blood mononuclear cells. Blood. 1996;88:3731–3740.

8. van der Loo J, Hanenberg H, Cooper R, Luo F-Y, Lazaridis E, Williams D. Nonobese diabetic/severe combined immunodeficiency (NOD/S-CID) mouse as a model system to study the engraftment and mobilization of human peripheral blood stem cells. Blood. 1998;92:2556–2570.
9. Roncarolo M, Carballido J, Rouleau M, Namikawa R, de Vries J. Human T-and B-cell functions in SCID-hu mice. Semin Immunol. 1996;8:207–213.
10. McCune J, Namikawa R, Kaneshima H, Shultz L, Lieberman M, Weissman I. The SCID-hu mouse: murine model for the analysis of human hematolymphoid differentiation and function. Science. 1988; 241:1632–1639.
11. Novelli E, Ramirez M, Leung W, Civin C. Human hematopoietic stem/progenitor cells generate CD5+ B lymphoid cells in NOD/SCID mice. Stem Cells. 1999;17:242–252.
12. Ito M, Hiramatsu H, Kobayashi K, et al. NOD/SCID/gamma(c)(null) mouse: an excellent recipient mouse model for engraftment of human cells. Blood. 2002;100:3175–3182.
13. Ito M, Kobayashi K, Nakahata T. NOD/Shi-scid IL2rgamma(null) (NOG) mice more appropriate for humanized mouse models. Curr Top Microbiol Immunol. 2008;324:53–76.
14. Kametani Y, Shiina M, Katano I, et al. Development of human-human hybridoma from anti-Her-2 peptide-producing B cells in immunized NOG mouse. Exp Hematol. 2006;34:1240–1248.
15. Matsumura T, Kametani Y, Ando K, et al. Functional CD5+ B cells develop predominantly in the spleen of NOD/SCID/gammac(null) (NOG) mice transplanted either with human umbilical cord blood, bone marrow, or mobilized peripheral blood CD34+ cells. Exp Hematol. 2003;34:1240–1248.
16. Saito Y, Kametani Y, Hozumi K, et al. Reconstitution of functional human B lymphocytes in NOD/SCID mice engrafted with ex vivo expanded CD34(+) cord blood cells. Int Immunol. 2002;30:1036–1043.
17. Ito R, Shiina M, Saito Y, Tokuda Y, Kametani Y, Habu S. Antigen-specific antibody production of human B cells in NOG mice reconstituted with the human immune system. Curr Top Microbiol Immunol. 2008;324:95–107.
18. Mansfield K. Marmoset models commonly used in biomedical research. Comp Med. 2003;53:383–392.
19. Mansfield K, Tardif S, Eichler E. White paper for complete sequencing of the common marmoset (Callithrix jacchus). 2004. Available at: http://www.genome.gov/Pages/Research/Sequencing/SeqProposals/MarmosetSeq.pdf. Accessed September 18, 2009.
20. Hibino H, Tani K, Ikebuchi K, et al. The common marmoset as a target preclinical primate model for cytokine and gene therapy studies. Blood. 2008;93:2839–2848.
21. Genain C, Abel K, Belmar N, et al. Late complications of immune deviation therapy in a nonhuman primate. Science. 1996;274:2054–2057.
22. Genain C, Hauser S. Experimental allergic encephalomyelitis in the new world monkey Callithrix jacchus. Immunol Rev. 2001;183:159–192.
23. LaBonte J, Babcock G, Patel T, Sodroski J. Blockade of HIV-1 infection of new world monkey cells occurs primarily at the stage of virus entry. J Exp Med. 2002;431:431–445.
24. Einspanier A, Lieder K, Bruns A, Husen B, Thole H, Simon C. Induction of endometriosis in the marmoset monkey (Callithrix jacchus). Mol Hum Reprod. 2006;12:291–299.
25. Massacesi L, Genain C, Lee-Parritz D, Letvin N, Canfield D, Hauser S. Active and passively induced experimental autoimmune encephalomyelitis in common marmosets: a new model for multiple sclerosis. Ann Neurol. 1995;37:519–530.
26. 't Hart B, Laman J, Bauer J, Blezer E, van Kooyk Y, Hintzen R. Modelling of multiple sclerosis: lessons learned in a non-human primate. Lancet Neurol. 2004;3:588–597.
27. Sasaki E, Suemizu H, Shimada A, et al. Generation of transgenic non-human primates with germline transmission. Nature. 2009;459:515–516.
28. Kohu K, Yamabe E, Matsuzawa A, et al. Comparison of 30 immunity-related genes from the common marmoset with orthologues from human and mouse. Tohoku J Exp Med. 2008;215:167–180.
29. Izawa K, Tani K, Nakazaki Y, et al. Hematopoietic activity of common marmoset CD34 cells isolated by a novel monoclonal antibody MA24. Exp Hematol. 2004;32:843–851.
30. Brok H, Hornby R, Griffiths G, Scott L, Hart B. An extensive monoclonal antibody panel for the phenotyping of leukocyte subsets in the common marmoset and the cotton-top tamarin. Cytometry. 2001;45: 294–303.
31. Marchler-Bauer A, Anderson J, Cherukuri P, et al. CDD: a conserved domain database for protein classification. Nucleic Acids Res. 2005; 33:192–196.
32. Song Y, Liu F, Zhang G, Liu D. Hydrodynamics-based transfection: simple and efficient method for introducing and expressing transgenes in animals by intravenous injection of DNA. Methods Enzymol. 2002; 246:92–105.
33. Ito R, Maekawa S, Kawai K, et al. Novel monoclonal antibodies recognizing different subsets of lymphocytes from the common marmoset (Callithrix jacchus). Immunol Lett. 2008;121:116–122.
34. McFarland H, Lobito A, Johnson M, et al. Effective antigen-specific immunotherapy in the marmoset model of multiple sclerosis. J Immunol. 2001;166:2116–2121.
35. Accardo-Palumbo A, Ferrante A, Cadelo M, et al. The level of Granzyme A is elevated in the plasma and in the Vgamma9/Vdelta2 T cell culture supernatants with active Behger's disease. Clin Exp Rheumatol. 2004;22(Suppl 34):S45–S49.
36. Amu S, Tarkowski A, Dorner T, Bokarewa M, Brisslert M. The human immunomodulatory CD25+ B cell population belongs to the memory B cell pool. Scand J Immunol. 2007;66:77–86.
37. Brisslert M, Bokarewa M, Larsson P, Wing K, Collins L, Tarkowski A. Phenotypic and functional characterization of human CD25+ B cells. Immunology. 2006;117:548–557.
38. Papayannopoulou B, Brice M, Broudy V, Zsebo K. Isolation of c-kit receptor-expressing cells from bone marrow, peripheral blood, and fetal liver: functional properties and composite antigenic profile. Blood. 1991;78:1403–1412.
39. Hogan C, Shpall E, McNulty O, et al. Engraftment and development of human CD34(+)-enriched cells from umbilical cord blood in NOD/LtSz-scid/scid mice. Blood. 1997;90:85–96.
40. Greiner D, Hesselton R, Shultz L. SCID mouse models of human stem cell engraftment. Stem Cells. 1998;16:166–177.
41. Wermann K, Fruehauf S, Haas R, Zeller W. Human-mouse xenografts in stem cell research. J Hematother. 1996;5:379–390.
42. Galy A, Morel F, Hill B, Chen B. Hematopoietic progenitor cells of lymphocytes and dendritic cell. J Immunother. 1998;21:132–141.
43. Okada S, Nakauchi H, Nagayoshi K, Nishikawa S, Miura Y, Suda T. In vivo and in vitro stem cell function of c-kit- and Sca-1-positive murine hematopoietic cells. Blood. 1992;80:3044–3050.

Vol 459|28 May 2009|doi:10.1038/nature08090

ARTICLES

Generation of transgenic non-human primates with germline transmission

Erika Sasaki[1], Hiroshi Suemizu[1], Akiko Shimada[1], Kisaburo Hanazawa[2], Ryo Oiwa[1], Michiko Kamioka[1], Ikuo Tomioka[1,3], Yusuke Sotomaru[5], Reiko Hirakawa[1,3], Tomoo Eto[1], Seiji Shiozawa[1,4], Takuji Maeda[1,4], Mamoru Ito[1], Ryoji Ito[1], Chika Kito[1], Chie Yagihashi[1], Kenji Kawai[1], Hiroyuki Miyoshi[6], Yoshikuni Tanioka[1], Norikazu Tamaoki[1], Sonoko Habu[7], Hideyuki Okano[4] & Tatsuji Nomura[1]

The common marmoset (*Callithrix jacchus*) is increasingly attractive for use as a non-human primate animal model in biomedical research. It has a relatively high reproduction rate for a primate, making it potentially suitable for transgenic modification. Although several attempts have been made to produce non-human transgenic primates, transgene expression in the somatic tissues of live infants has not been demonstrated by objective analyses such as polymerase chain reaction with reverse transcription or western blots. Here we show that the injection of a self-inactivating lentiviral vector in sucrose solution into marmoset embryos results in transgenic common marmosets that expressed the transgene in several organs. Notably, we achieved germline transmission of the transgene, and the transgenic offspring developed normally. The successful creation of transgenic marmosets provides a new animal model for human disease that has the great advantage of a close genetic relationship with humans. This model will be valuable to many fields of biomedical research.

The use of transgenic mice has contributed immensely to biomedical science. However, the genetic and physiological differences between primates and mice—including their neurophysiological functions, metabolic pathways, and drug sensitivities—hamper the extrapolation of results from mouse disease models to direct clinical applications in humans. Thus, the development of non-human primate models that mimic various human systems would accelerate the advance of biomedical research. In particular, genetically modified primates would be a powerful human disease model for preclinical assessment of the safety and efficacy of stem-cell or gene therapy.

The common marmoset (*Callithrix jacchus*) is a small New World primate that, because of its size, availability, and unique biological characteristics[1], has attracted considerable attention as a potentially useful biomedical research animal in fields such as neuroscience, stem cell research, drug toxicology, immunity and autoimmune diseases, and reproductive biology. Marmosets have a relatively short gestation period (about 144 days), reach sexual maturity at 12–18 months, and females have 40–80 offspring during their life. Therefore, the application of transgenic techniques to marmosets may be feasible, and would greatly facilitate the study of human disease. In contrast, the more commonly used Old World primates, such as the rhesus monkey (*Macaca mulatta*) and cynomolgus monkey (*Macaca fascicularis*), show slow sexual maturation (about 3 years) and have fewer offspring (around 10) over the female lifespan. Thus, even though marmosets are less closely related to humans than either apes or Old World primates, their potential as transgenic primate models of human disease means they may be uniquely valuable.

Obtaining large numbers of oocytes from primates for transgenic experiments is limited by ethical and economic constraints. However, because retroviral vectors allow the efficient integration of a provirus into the host genome[2–4], their use requires fewer oocytes than some other techniques. Furthermore, the injection of a lentiviral vector into the perivitelline space of a pre-implantation embryo, which is less invasive than injection into the pronucleus, is an advantageous method for generating transgenic animals. In fact, transgenic modification of rhesus monkeys using retroviral vectors and a lentiviral vector[5–7] has been attempted. In these studies, genomic integration and expression of the transgene was observed in the placenta, but not in the infants' somatic tissues, by objective analyses such as PCR with reverse transcription (RT–PCR) or western blotting.

The recombinant adeno-associated virus has been used for the targeted knockout of the cystic fibrosis transmembrane conductance receptor gene in swine fetal fibroblasts, and targeted gene knockout pigs have been generated by somatic cell nuclear transfer (SCNT) of the fibroblast nuclei into oocytes[8,9]. Although conceptually this method could be used to make targeted gene-knockout primates, marmoset SCNT techniques are not available at present.

Here we successfully produced transgenic marmosets, by injecting a lentiviral vector containing an enhanced green fluorescent protein (EGFP) transgene[10] into marmoset embryos. Four out of five transgenic marmosets expressed the EGFP transgene in neonatal tissues; the fifth expressed it in the placenta. Two showed transgene expression in the germ cells, and one fathered a healthy transgenic neonate. Our method for producing transgenic primates promises to be a powerful tool for studying the mechanisms of human diseases and developing new therapies.

Production of transgenic marmosets

In a pilot study, we showed that pre-implantation marmoset embryos obtained through natural intercourse had much better developmental potential than embryos obtained by *in vitro* fertilization (IVF). Therefore, both natural and IVF embryos were used in this study.

[1]Central Institute for Experimental Animals, 1430 Nogawa, Miyamae-ku, Kawasaki, Kanagawa 216-0001, Japan. [2]Department of Urology, Juntendo University Nerima Hospital 3-1-10 Takanodai, Nerima-ku, Tokyo 177-8521, Japan. [3]Center for Integrated Medical Research, [4]Department of Physiology, Keio University School of Medicine, 35 Shinanomachi, Shinjuku-ku, Tokyo 160-8582, Japan. [5]Natural Science Centre for Basic Research and Development, Hiroshima University 1-2-3, Kasumi, Minami-ku, Hiroshima 734-8551, Japan. [6]Subteam for Manipulation of Cell Fate, RIKEN BioResource Centre, 3-1-1 Koyadai, Tsukuba, Ibaraki 305-0074, Japan. [7]Department of Immunology, Tokai University School of Medicine, Bohseidai, Isehara, Kanagawa 259-1193, Japan.

To introduce the EGFP gene into the marmoset embryo, three kinds of self-inactivating lentiviral vectors were constructed on the basis of human immunodeficiency virus type 1 (HIV-1), and each carried a different promoter, CAG, CMV or EF1-α. The self-inactivating lentiviral vectors were named CAG-EGFP, CMV-EGFP and EF1-α-EGFP, respectively.

All lentiviral vector injections were performed at the earliest embryonic stage possible using an Eppendorf FemtoJet express and a Narishige micromanipulator. Twenty-seven IVF embryos and 64 natural embryos were injected with a high titre of the lentiviral vector, from 5.6×10^9 to 5.6×10^{11} transducing units per ml (Table 1). Because the perivitelline space of the marmoset early embryo is rather small, 16 of the 27 IVF embryos, and 49 of the 64 natural embryos, at the pronuclear-to-morula stage, were first placed in 0.25 M sucrose in PBI medium (0.25 M sucrose medium), which made the perivitelline space expand 1.2–7.5-fold (data not shown). The lentiviral vector was then injected into the perivitelline space (Supplementary Data 1). Virus was injected into the blastocoel of the remaining 11 IVF and 15 natural embryos at the blastocyst stage, without the 0.25 M sucrose treatment (Supplementary Data 1).

Immediately after injection, 4 of the IVF and 12 of the natural embryos were transferred to recipient females. The rest were examined for the expression of EGFP, starting 48 h after injection. Among the sucrose-treated IVF and natural early embryos at 48 h after injection, 68.8% and 97.7% expressed EGFP, respectively; of the non-sucrose-treated IVF and natural embryos injected with lentivirus as blastocysts, 85.7% and 87.5% expressed EGFP, respectively (Supplementary Data 1). Therefore, 61 of the natural embryos and 19 of the IVF embryos were transferred to surrogate mothers (Table 1). For the transfers, the recipients were synchronized with the donor oocyte cycle; each recipient received 1–3 embryos per cycle, and 50 surrogate mother animals were used.

Of the surrogate mothers, seven that received natural or IVF embryos became pregnant. Three recipients miscarried on days 43, 62 and 82, and the other four delivered five healthy offspring (three singletons, one pair of twins), one male (number 666) and four females, on days 144–147 after ovulation (Fig. 1). For the infants, the lentiviral vector injection had been performed at the four-cell stage (584), the pronuclear stage (587), and the morula stage (588, 594 and 666). The EGFP transgene was driven by the CAG promoter in three newborns (584, 587 and 588) and by the CMV promoter in the other two (594 and 666; Supplementary Data 1).

Table 1 | Production rates of transgenic marmosets

	Artificial reproductive technique	Natural
Number of GV oocytes	460	No data
Number of matured oocytes (only MII)	201	No data
Number of IVFs performed (including MI)	272	No data
Number of fertilized oocytes	121	No data
Fertilization rate (fertilization per GV)	26.3%	No data
Fertilization rate (fertilization per IVF)	44.5%	No data
Lentiviral injections	27	64
EGFP expression confirmed after 48 h or later	23	52
EGFP expression	17	50
EGFP expression rate	73.9%	96.2%*
ETs	19	61
Number of surrogates	13	37
Number of pregnancies	1	6
Number of deliveries	1	3
Births	1	4
Birth rate (birth per ET)	5.20%	6.55%
Number of Tgs	1	4
Production rate (Tg per injection)	3.70%	6.25%
Production rate (Tg per ET)	5.26%	6.25%
Production rate (Tg per birth)	100	100

ET, embryo transfer; GV, germinal vesicle; MI, metaphase I; MII, metaphase II; Tg, transgenes. *$P < 0.01$, chi-squared analysis.

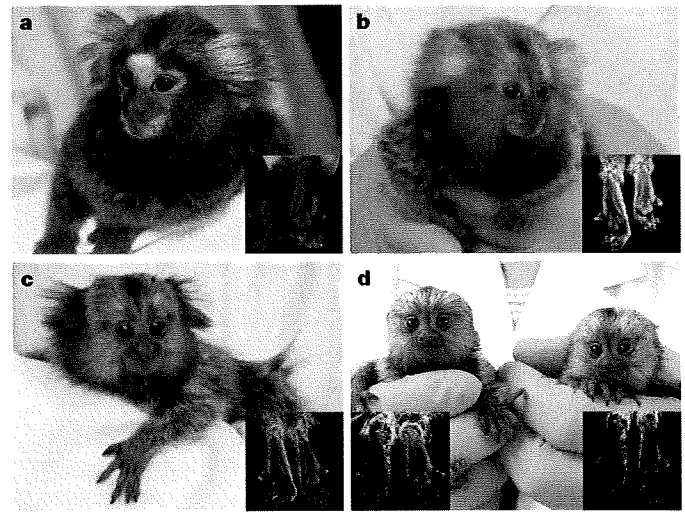

Figure 1 | Self-inactivating lentiviral vector-derived EGFP transgenic marmosets. a–d, The transgenic marmoset infants are shown. Shown are 584 (Hisui) (**a**), 587 (Wakaba) (**b**), 588 (Banko) (**c**), and twin infants 594 (Kei)/666 (Kou) (**d**). 584, 587 and 588 contained CAG-EGFP and 594/666 carried CMV-EGFP. Inset boxes in each panel show epifluorescent images of the paw of a transgenic animal (right), compared to a wild-type animal's foot pad (left). All animals except 588 expressed EGFP in their paw. 666 expressed EGFP at a slightly lower level.

EGFP transgene integration in the genome

The integration, transcription and expression of the transgene in the infant marmosets were examined using tissues that could be acquired noninvasively (placenta, hair roots, skin and peripheral blood cells). Because marmosets usually eat the placenta after delivery, only three placentae (584, 588 and that shared by twins 594/666) were collected and available for analysis[11].

The placental DNA from infants 584 and 588 showed high levels of the transgene content by real-time PCR, whereas that from 594/666 showed a relatively low level (Supplementary Data 2). The transgene was detected in the hair roots, skin and peripheral blood from infants 584, 587, 594 and 666.

Copy numbers of the integrated transgene were determined by Southern blotting analysis. At least four copies of the transgene were integrated into the genome of animal 584, and two copies were present in the genome of animal 587 (Fig. 2). Several integration sites in the genomic DNA of skin fibroblast cells, peripheral blood, the placenta of 594 and 666, and the placenta of 588 were found. Infant 588 showed transgene integration only in the placenta (Fig. 2).

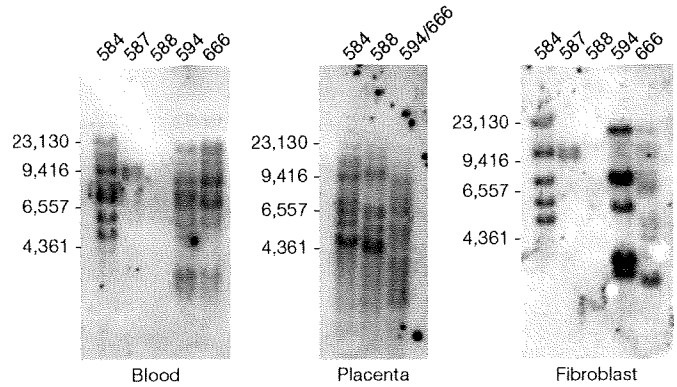

Figure 2 | Transgene insertions in several infant tissues. Southern blot analysis. All infants except 588 showed transgene integration in the skin fibroblast cells and blood, whereas 588 showed transgene integration in the placenta. The lane markers on the left of each gel represent base pairs.

To identify the chromosomal transgene integration sites, fluorescence *in situ* hybridization (FISH) was performed. Consistent with the Southern blotting analysis, the FISH results showed several integration sites in the chromosomes of peripheral blood mononuclear cells (MNCs), and further showed that each infant had different transgene integration patterns with patterns the sometimes varied among different MNCs (Supplementary Fig. 1 and Supplementary Data 3). In 584, four transgene integration sites were seen, on chromosomes 2, 7 and 13; in 587, two distinct signals were recognized in the peripheral blood lymphocyte DNA, on chromosomes 3 and 12. No signal was detected in the peripheral blood lymphocyte samples from 588, and several transgene integration patterns were seen in 594 and 666. Infant 594 had at least three different transgene integration patterns, and more than six patterns may have occurred. Infant 666 showed the largest number of integration patterns, up to 13. Moreover, although this animal was male, of the 13 investigated karyograms, eight samples were of the female karyotype, owing to haematopoietic chimaerism caused by blood exchange with his twin, 594.

Expression of the EGFP transgene

EGFP messenger RNA was detected in the hair roots of all the infants except 588 and in the peripheral blood cells of 584 and 587, by RT–PCR. Transcription of the EGFP gene was indicated in all of the placental samples, 584, 588 and 594/666 (Fig. 3a–c).

To assess EGFP expression in tissues, EGFP fluorescence was examined directly by fluorescence microscopy, and immunohistochemical analysis of the hair roots, frozen sections of a small piece of ear tissue, and placenta samples was performed (Fig. 3d–g). EGFP was strongly expressed in the epidermal cells of the ear tissue and stromal cells of the placenta. In all of the animals except 588, EGFP expression was observed in the hair roots and skin. Placental samples from 584 and 588 also showed high levels of EGFP, but it was undetectable in 594/666 (Supplementary Figs 2–4).

Peripheral blood samples were subjected to flow cytometric analysis using a FACScant. FACS analysis showed EGFP-positive peripheral blood MNCs in 584 and 587. The proportion of EGFP-positive cells was 15.7 and 19.1%, respectively (Fig. 3h). The flow cytometry results corresponded well with those from RT–PCR. Among the peripheral blood cells, the EGFP-positive percentage of granulocytes, lymphocytes and monocytes was 34.5, 3.3 and 18.0% in 584, and 47.7, 4.6 and 20.0% in 587, respectively (Supplementary Fig. 5).

Germline transmission of the transgene

At the moment when two of the animals (666 and 584) became sexually mature, the transgene expression in their gametes was analysed. Semen samples were collected from 666, and live spermatozoa were obtained by the swim-up method in TYH medium. RT–PCR analysis demonstrated the presence and expression of the transgene in the germ cells of 666 (Fig. 4a). IVFs were then performed using semen collected from 666 and wild-type oocytes to analyse the fertility of the germ cells carrying the transgene. Fluorescence microscopy showed that 20–25% of the IVF embryos strongly expressed EGFP, as shown in Fig. 4b. Furthermore, three pre-implantation live natural embryos were collected from female animal 584, and one of these embryos strongly expressed EGFP. The IVF embryos from 666 and two of the natural blastocyst embryos from 584 were shown to express the EGFP transgene by RT–PCR (Fig. 4a). Three EGFP-positive IVF embryos from the male animal (666) were then transferred into a surrogate mother. One neonate (687) was delivered at full term by caesarean section, and this neonate carried the EGFP gene and expressed the transgene in skin (Fig. 4c–e), but not in the placenta and hair.

Discussion

To our knowledge, this is the first report of transgenic non-human primates showing not only the transgene expression in somatic tissues, but also germline transmission of the transgene with the full, normal

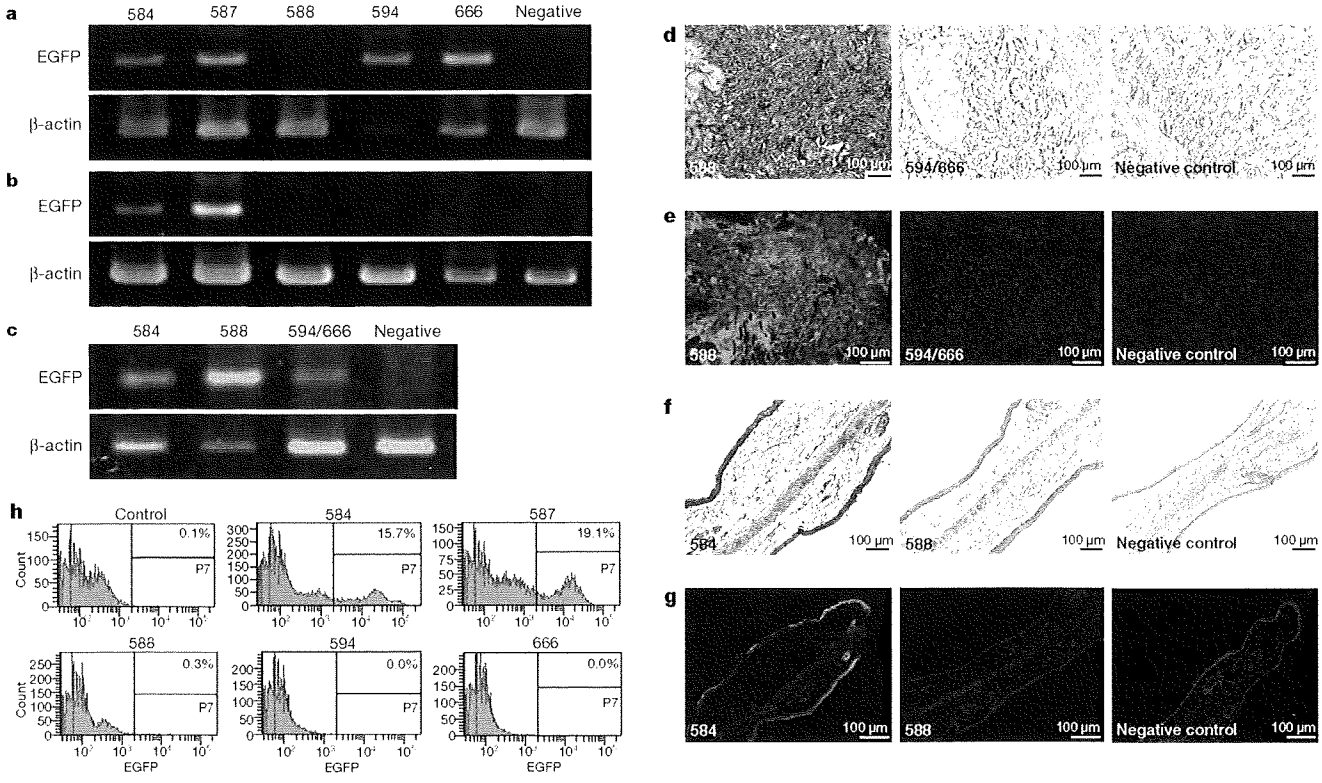

Figure 3 | Transgene transcription and expression in several infant tissues. **a**–**c**, RT–PCR results from hair roots (**a**), peripheral blood (**b**) and placenta (**c**). Each lane indicates the animal number. **d**–**g**, Immunohistochemical (**d**, **f**) and epifluorescence (**e**, **g**) analyses using an anti-EGFP antibody, of frozen ear tissues (**f**, **g**) and placentae (**d**, **e**). Scale bars, 100 μm. **h**, Results of FACS analysis using whole peripheral blood cells. The percentage of EGFP-positive cells is shown in the top right of each panel.

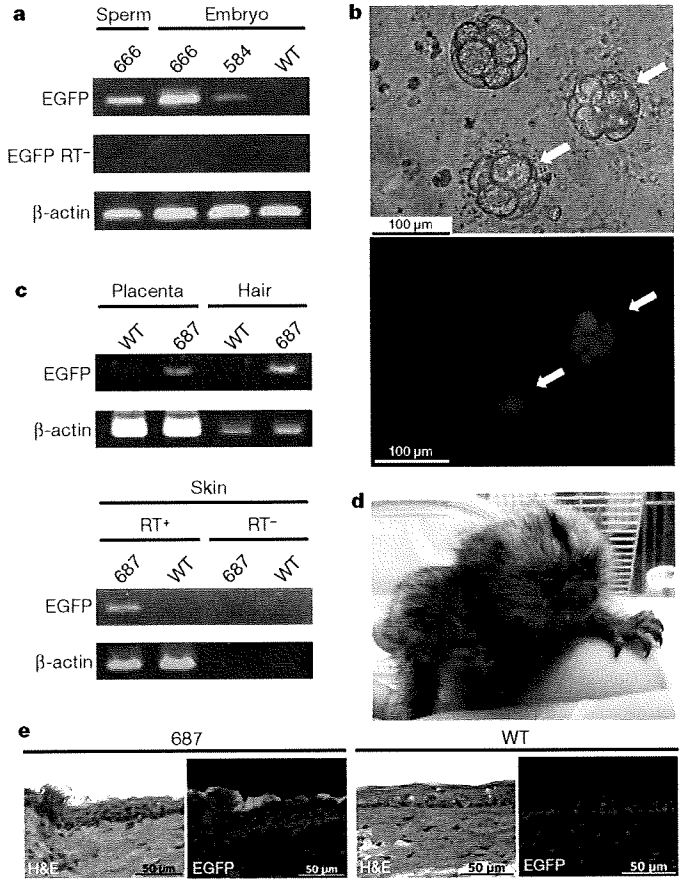

Figure 4 | Germline transmission of the transgene. **a**, RT–PCR analysis of spermatozoa and IVF embryos from 666, and natural embryos from 584. RT− denotes the absence of reverse transcriptase as a control. **b**, Bright-field and dark-field of epifluorescence images of IVF embryos. EGFP-positive IVF embryos produced with 666 spermatozoa are indicated by white arrows. **c**, PCR (top panel) and RT–PCR (bottom panel) analysis of the tissues from the F_1 neonate. **d**, Photograph of the F_1 offspring (687) from 666. **e**, Haematoxylin and eosin (H&E) staining and epifluorescence imaging of frozen skin tissue from the neonate. WT, wild-type control.

development of the embryo. We obtained five transgenic marmosets, four of which expressed the transgene in several somatic cell lineages, such as hair root, skin fibroblast and peripheral blood cells. The remaining animal expressed the transgene only in the placenta. Two of these animals reached sexual maturity and showed the transgene insertion and expression in germ cells. Epifluorescence microscopic observation and RT–PCR analysis of embryos generated by transgene-bearing gametes strongly indicated that the transgenic germ cells from animals 666 and 584 were fertile, and this was proved for the male (666) who fathered one healthy, transgenic infant (687) with the transgene expression in the somatic cells. These findings suggest that it should be possible to establish transgenic non-human primate colonies, opening the door to their use in biomedical research.

Because the manipulation of embryos for viral injection and their subsequent culture may affect embryonic development, the birth rate after embryo transfer (6.25%) was lower than that for normal embryos (30.7%, data not shown). The miscarriage rates were not significantly different between embryonic transfers performed using normal embryos (28.6%) and transgenic embryos (42.6%). Despite considerable effort, transgenic marmosets have not been produced by DNA pronuclear microinjection. The production rate that we obtained using lentivirus (5.26–6.25%) suggests that our technique is sufficiently effective for the production and use of genetically modified marmosets as human disease models.

The 100% birth rate of transgenic marmosets achieved in the present study could be due to several technical advantages. First, we used EGFP as the transgene, enabling us to monitor the presence and expression of the transgene at each experimental step in live embryos and the transgenic animals. Accordingly, we were able to select unambiguously EGFP-expressing embryos for transfer into surrogate mothers. This selection was effective, not only for increasing the birth rate of transgenic animals, but also for reducing the number of surrogate mother animals needed.

Second, we used pre-implantation embryos obtained by natural intercourse, high-titre lentiviral vectors, and 0.25 M sucrose solution as a medium for injection. Even though the birth rates (birth per embryonic transfer) were no different between IVF and natural embryos, the fertilization rate of the germinal vesicle-stage oocytes was quite low. Because it is difficult to collect large quantities of oocytes, it was advantageous to use marmoset natural embryos. To inject as much lentiviral vector as possible into the perivitelline space, the embryos were placed in 0.25 M sucrose medium at the time of lentiviral vector injection, which expanded the volume of the perivitelline space 1.2–7.5-fold. For example, the estimated volume of the perivitelline space of one marmoset pronuclear stage embryo was approximately 31.5 pl, but when placed in 0.25 M sucrose medium, it expanded to about 231 pl. A high titre of the lentiviral vector solution was used so that many lentiviral vector particles were injected into the expanded perivitelline space; approximately 1.3×10^3–1.3×10^5 transducing units of lentiviral vector were injected in this study. Each of these steps probably contributed to the successful production of transgenic marmosets.

The high number of injected lentiviral vector particles resulted in several transgene integrations, as observed by Southern blot analysis and FISH. The embryos injected with the transgene before the four-cell stage (584 and 587) showed fewer than four copies of the transgene per genome by Southern blotting and FISH. The three other embryos (588, 594 and 666), which received the injection at the morula stage, exhibited several integrations of the transgene by Southern blotting and FISH. As the FISH analysis was performed using only peripheral blood MNCs, other patterns of transgene integration cells may have existed in other tissues. The FISH results for 666 were consistent with this hypothesis, as the integration sites in the chimaeric blood MNCs from his twin, 594, were different from those in the blood MNCs of 594.

The lentiviral vector used in the present study can be used to transmit only relatively small transgenes, 8.5 kilobases of DNA or less. Therefore, further study will be necessary to enable the introduction of larger transgenes into marmoset embryos. Furthermore, to study human diseases involving the malfunctions of specific genes, targeted gene-knockdown marmosets could be developed using RNA interference (RNAi) lentiviruses.

The results of the present study indicate that transgenic marmosets may be used as experimental animals for biomedical research. Recently, somatic cell nuclear-transferred embryonic stem cells from the rhesus macaque and induced pluripotent stem cells from adult human fibroblasts were reportedly established[12–15]. Those studies indicated that the obstacle caused by immunogenetic incompatibility has at least theoretically been resolved, and that a new era of regenerative medicine using somatic cell nuclear-transferred embryonic stem cells in primates[14] or human induced pluripotent stem cells[12,13,15] has become possible. However, before such stem cells can be used in clinical applications, preclinical assessments of their safety and efficacy are essential. We previously reported that marmosets with injured spinal cords can recover motor function after the transplantation of human neural stem/progenitor cells[16], highlighting the usefulness of the marmoset for assessing the safety and efficacy of, not only these cells, but also of other stem cells, such as human embryonic stem cells[17] or induced pluripotent stem cells. Human disease models in non-human primates have so far been limited to mechanical injury models (for example, spinal cord injury[18]) and drug administration models (for example, MPTP-induced Parkinson's[19,20]). The only transgene-induced primate disease model is of Huntington's disease[7], in rhesus